

REMARKS

Overview

In the non-final Office Action under reply, claims 23-28 and 61-62 were examined, claims 1-22 and 29-60 having been withdrawn as directed to non-elected subject matter. Applicants acknowledge with appreciation the Examiner's withdrawal of the obviousness-type double patenting rejection of claims 23-28, as well as the rejection under 35 U.S.C. § 102(a) or § 102(e) of claims 23-28, as well as the rejection under 35 U.S.C. § 103(a) of claim 26 as set forth in the previous Office Action dated March 9, 2007.

Claims 23-28, 61, and 62 have been rejected under 35 U.S.C. §103(a) as unpatentable over by Matyjaszewski et al., USPN 6,627,314 ("Matyjaszewski") in view of Milstein, USPN 5,820,881 ("Milstein"). The rejection is traversed for at least the reasons set forth below.

Rejection under 35 U.S.C. §103(a)

Claims 23-28, 61, and 62 stand rejected under 35 U.S.C. §103(a) as unpatentable over by Matyjaszewski in view of Milstein. This rejection is traversed.

The teachings of Matyjaszewski have been discussed previously. See applicants' remarks set forth in the response dated September 10, 2007, which are incorporated herein by reference. In summary, Matyjaszewski is directed at the preparation of *nanocomposite* structures (see, for example, the title of Matyjaszewski). Accordingly, Matyjaszewski is directed entirely to the preparation of nanoscale materials. The nanoscale materials of Matyjaszewski are prepared using a controlled/living polymerization process, wherein initiation of the polymerization occurs from initiator sites disposed on an inorganic colloid (Matyjaszewski at col. 1, lines 16-19). Matyjaszewski provides no disclosure that would guide the skilled artisan in preparing the presently-claimed materials. The Action states:

It would be prime facie obvious to a person of ordinary skill in the art at the time of the invention to make or use larger microparticles than those exemplified in Maty, especially if the microspheres were designed for drug delivery. The motivation comes from Milstein, who teaches that particles from 0.2 microns to 10 microns are most suitable for drug delivery. This substantially overlaps instant claims, which require, in their most limited aspect (claim 61) a size between 3 and 10 microns.

(Action at 3.) Applicants disagree.

First, applicants note that Milstein discloses diamide-dicarboxylic acid microspheres (see, for example, Milstein at col. 2, lines 17-18). The microspheres disclosed in Milstein are prepared

using chemistry that differs dramatically from the procedures used in Matyjaszewski. The diamide-dicarboxylic acid microspheres of Milstein are prepared by a two step process: (A) solubilizing a diamide-dicarboxylic acid to yield a first solution; and (B) contacting the first solution with a precipitator solution in which the diamide-dicarboxylic acid is insoluble (see Milstein at col. 2, lines 47-52). Additional synthetic information for preparing the microspheres is presented in cols. 5-6 of Milstein. In general, the microspheres are prepared using a self-assembly mechanism (see, for example, Milstein at col. 5, lines 56-57, or col. 6, lines 2-3, or col. 6, lines 14-15). The microspheres of Milstein do not involve polymerization reactions of any type, and particularly do not involve the radical-type polymerization mechanisms described in Matyjaszewski. In fact, Milstein mentions polymerization only twice: (1) in the Background section to describe prior art (Milstein at col. 1, lines 57-59); and (2) in Example 19, where polymerization is carried out to allow the microspheres to be imaged by TEM (Milstein at col. 17, lines 23-32).

In light of the significant differences between the chemical processes disclosed in Matyjaszewski and in Milstein, the skilled artisan would not look to Milstein when seeking to modify the nanoparticles disclosed in Matyjaszewski. The single experimental reference in Milstein to polymerization of microparticles (i.e., Milstein's Example 19) relates to preparing pre-formed microparticles for analytical measurement, not to actually forming the microparticles using a polymerization reaction. Furthermore, Milstein makes no reference whatsoever to controlled polymerizations, polymerizations from surface-tethered initiator sites, or radical polymerizations, which are the subject of Matyjaszewski. In essence, apart from the broad concept of "making particles," the methods of Milstein have no relationship whatsoever to the methods of Matyjaszewski. One of skill in the art would find no motivation in Matyjaszewski to consult Milstein, nor would the skilled artisan find motivation in Milstein to consult Matyjaszewski.

Even if, *arguendo*, the skilled artisan looked to Milstein for motivation to prepare particles larger than those disclosed in Matyjaszewski, Milstein provides no teachings that would help the skilled artisan overcome the significant technological problems that would be encountered in such an endeavor. The Action states:

To the extent that Maty only specifically teaches particle sizes up to 1 micron, note that in the art of making microscopic particles, the technical challenges are associated with decreasing, not

increasing, the particle size. Thus the artisan would enjoy a reasonable expectation of success at making particles like those of Maty but with a larger diameter.

(Action at pp. 3-4.) Applicants respectfully disagree. While it may be true that miniaturization of many processes is more difficult than enlarging such processes, this is not necessarily true for the preparation of microparticles and nanoparticles. In fact, the difficulties encountered in making nanoparticles are quite different from those encountered in making microparticles, and a process that works well for one may require significant modification in order to work well for the other.

For example, it is well known that larger particles have a proportionately smaller amount of atoms located at the particle surface compared with smaller particles. (See, for example, page 429 of Fendler et al., Nanoparticles and Nanostructured Films, Wiley, NY (1999), pp 429-461, attached hereto as Appendix A.) This is a crucial consideration for enlarging the processes disclosed in Matyjaszewski, since Matyjaszewski prepares particles by initiating polymerization reactions on the surface of core particles. A larger core particle has relatively fewer initiator sites compared with the amount of material forming the internal portion of the core particle. In fact, it is a great challenge to obtain significant polymer density on the surface of microparticle scaffolds, because (1) a large number of initiator sites must be present on the surface of the microparticle, and (2) a large percentage of such initiator sites must actually initiate polymerization. If any appreciable areas of the microparticle surface do not have initiator sites, or if any appreciable percentage of initiator sites do not initiate polymerization, the microparticle will have areas of the surface that are not covered by polymer. In contrast, nanoparticles may have thick and relatively uniform polymer shells even when few surface-bound initiator sites are present and/or initiate polymerization. Growing polymers from surface initiator sites to form polymer shells on particles (the so-called "grafting-from" method) therefore increases in difficulty as the size of the particle increases. Matyjaszewski addresses none of these issues, and even if one of skill in the art found motivation to prepare microparticles from the disclosure of Matyjaszewski or Milstein, the skilled artisan would have no expectation of success because Milstein provides no disclosure that would help the skilled artisan overcome these difficulties.

The traditionally-held view that miniaturization of a process is more difficult than enlarging the same process is frequently correct for macroscopic processes. The nanometer-scale processes disclosed by Matyjaszewski, however, operate essentially on the molecular level. The "grafted-from" type of polymerizations that occur on the colloidal particles of Matyjaszewski


require specific control of surface atoms on the particles. Enlarging a process that occurs on the molecular level cannot be assumed *prima facie* obvious any more than one would consider it *prima facie* obvious to convert a macroscopic process to a molecular level process.

The MPEP provides the standard required for a *prima facie* case of obviousness: "the examiner must provide evidence which as a whole shows that the legal determination sought to be proved (i.e., the reference teachings establish a *prima facie* case of obviousness) is more probable than not." (MPEP § 2142.) The processes taught in Matyjaszewski and those taught in Milstein are both related to "making particles." There the similarities end between these references, and the processes neither combine nor supplement each other to arrive at the methods of the pending claims. Furthermore, the significant difficulties that the skilled artisan would encounter in attempting to modify the teachings of Matyjaszewski to arrive at the methods of the instant claims are neither discussed nor overcome by the teachings of the cited references. Accordingly, there is not a preponderance of evidence to support the conclusion that the instant claims are *prima facie* obvious over the references. Withdrawal of the rejection is respectfully requested.

CONCLUSION

Applicants submit that the claims of the application are in condition for allowance. Applicants respectfully request withdrawal of the rejections, and prompt issuance of a notice of allowance. If the Examiner has any questions concerning this communication, or would like to discuss the application, the art, or other pertinent matters, a telephone call to the undersigned would be welcomed.

Respectfully submitted,

By: 
Isaac M. Rutenberg
Registration No. 57,419
c/o MINTZ LEVIN
1400 Page Mill Road
Palo Alto, California 94304-1124
(650) 251-7700 Telephone
(650) 251-7739 Facsimile
Customer No. 23980

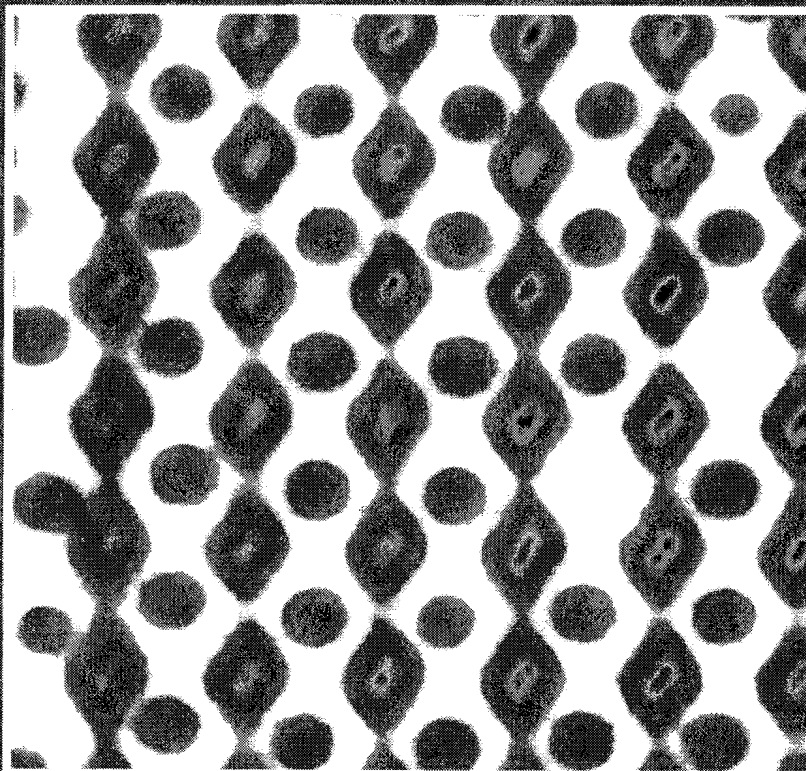
Appendix A

Fendler et al., Nanoparticles and Nanostructured Films, Wiley, NY (1999), pp 429-461.

Nanoparticles and Nanostructured Films

Preparation, Characterization
and Applications

edited by Janos H. Fendler



Chapter 18

Nanoparticles and Nanostructured Films: Current Accomplishments and Future Prospects

J. H. Fendler and Y. Tian

18.1 Introduction

Properties of solid materials undergo drastic changes when their dimensions are reduced to the nanometer size regime. For semiconductors this transition occurs when the particle sizes are comparable to the de Broglie wavelength of the electron, to the mean free path of the exciton, or to the wavelength of the phonons. Particles in the nanometer range, i.e., nanoparticles, are said to be size quantized. Size-quantized particles are prepared by both physical and chemical methods. The more traditional approach involves physical processing (grinding or ball-milling of larger particles, crystal growing, ion implantation, and molecular epitaxy, for example) rather than chemical syntheses. Advantage, on the other hand, is taken of versatile inorganic, organic, and electrochemical synthetic methodologies in the chemical approach to construct nanoparticles with distinct electronic structures from their constituent atoms and molecules, and crystal and surface structures from their bulk materials. Additionally, preparative, polymer, and colloid chemical techniques are employed to control the sizes and monodispersities of the incipient nanoparticles and to stabilize them in the solid state and in aqueous and nonaqueous dispersions [1, 2]. Significantly, biomineralization, mother nature's construction of nanoparticles in cells [3, 4], has inspired many nanoparticle preparations [5, 6].

The unique properties of metallic, semiconducting, magnetic, and ferroelectric nanoparticles have prompted the burgeoning interest in these systems. The size-dependent behavior of nanoparticles manifests itself in markedly altered physical and chemical behavior. In particular, changes in mechanical, optical, electrical, electro-optical, magnetic, and magneto-optical properties have been investigated [7-10].

It is important to keep in mind that the smaller the particles are, the larger the portion of their constituent atoms are located at the surface. For example, in a 2 nm-diameter gold (or CdS) particle, approximately 60% of the atoms (or molecules) are located at the surface. In semiconductors, this arrangement facilitates electron and/or hole transfers to and from acceptors and/or donors localized at the

nanoparticle surface. In metallic nanoparticles, a large surface-area-to-volume ratio permits effective charge transfer and elicits charge-transfer-dependent changes in the optical absorption spectra [11]. It is becoming increasingly recognized that the properties of nanoparticles are strongly influenced by the physics and chemistry of their surface states. The surface states, in turn, are affected by the crystal morphology of the nanoparticles, by the chemicals attached to them (capping reagents, for example [12]), and by the media which surround them [13].

Nanoparticle research has reached a well-deserved maturity. Ample summaries, reviews, and books document the accumulated information [14, 15]. Nanoparticle research continues to be the subject of national and international symposia and workshops [16]. The current state of the art activities focus upon treating nanoparticles as large macromolecules and linking them, by electrostatic interactions or covalent bonds, into heterostructured supramolecules, two-dimensional arrays, or three dimensional networks. Alternatively, and additionally, nanoparticles are being self-assembled to hierarchically more complex structures [17]. The integration of nanoparticles into nanostructured films has, in fact, been reflected in many of the chapters assembled in the present volume.

The goals of the present closing chapter are (i) to summarize the current activities in nanoparticle preparations, (ii) to enable the neophyte to launch desired experiments by providing data on the properties of the most frequently used bulk semiconductors and on the preparation and characterization of the corresponding nanoparticles, and (iii) to speculate on future research directions related to nanoparticles and nanostructured films.

18.2 Preparations of Nanoparticles and Nanostructured Films: Current State of the Art

18.2.1 Definitions

Strictly speaking, nanoparticles are uniformly constituted from identical atoms or molecules, nonagglomerated and monodisperse in some liquid. In reality, they often agglomerate into larger irregular entities and are rarely monodispersed. Chemically prepared nanoparticles seldom have uniform purity. Furthermore, nanoparticles are stabilized by surfactants or large polyions or are embedded in some matrix. This, inevitably, alters their surface states.

Deposition or transfer of the nanoparticles to solid support results in the formation of nanoparticulate (nanostructured) films in which the thickness, the packing density, and the orientation of the nanoparticles are potentially controllable. Nanoparticulate films are interesting since they are size quantized even though the individual nanoparticles are in physical contact with each other. Thus, lateral conductivity becomes measurable in nanostructured films prepared from conducting or semiconducting materials.

18.2.2 Chemical Preparations of Nanoparticles

Metallic, semiconducting, and magnetic nanoparticles have been prepared in a wide variety of different media by wet chemical techniques. The available literature, up to 1992, has been summarized in a recent review [5]. More recent developments in semiconductor nanoparticle preparations are surveyed (albeit not exhaustively) in Tables 18.1–18.6. The salient features that appear from these tables are as follows.

- The preparation of highly monodisperse colloidal semiconductor nanoparticle dispersions has become a routine matter [18–22]

In a benchmark method 13, 14, 16, 19, and 23 Å-diameter CdS nanoparticles were prepared as fully redispersible powders [19]. The method involved the addition of H₂S to a vigorously stirred aqueous solution of Cd(ClO₄)₂ · 6H₂O (1.97 g, 4.70 mmol) and 1-thioglycerol (1 mL, 11.53 mmol), adjusted to pH = 11.2 (1 M NaOH). The desired size of CdS nanoparticles was obtained by the judicious control of the quantity of H₂S introduced and by changes of the temperature. Low-molecular-weight contaminants were removed by dialysis. Replacing the perchlorate anion by acetate or nitrate ions had a profound influence on the mean diameters of the nanoparticles produced [19]. In an alternative and versatile method, injection of appropriate organometallic reagents into a hot coordinating solvent (tri-*n*-octylphosphine, TOP) led to the production of nearly monodisperse CdS, CdSe, and CdTe [20]. Production of monodispersed particles is believed to be the consequence of a temporary discrete nucleation, attained as the consequence of an abrupt supersaturation (upon reagent injection) and a subsequent controlled particle growth by Ostwald-ripening. Typically, nanoparticles are stabilized by bulky anions (hexametaphosphate, for example), by polyions (polyvinyl alcohol, for example), or by capping by nucleophilic reagents (thiophenol, for example). The function of the capping agent is to inhibit the nanoparticle growth at the desired size and to ensure monodispersity [20]. Importantly, given populations of nanoparticle dispersions can be dried and stored as solids. The solid nanoparticles can then subsequently be redispersed without any alteration of their sizes and size distributions.

- Size-selected precipitation provides a convenient means for producing monodisperse nanoparticles [18–20].

Advantage is taken in size-selected precipitation of preferential flocculation of the larger nanoparticles by increasing the polarity of the dispersing liquid. Enhancing the polarity of the media reduces the attractive forces between the nanoparticles and the larger particles experience the greatest change in interparticle interactions and thus they precipitate first. This results, in turn, in a narrowing of the size distribution of the nanoparticles, which remain in the supernatant. Size-selected precipitation has been successfully employed, for example, for the isolation of highly monodisperse 6.4, 7.2, 8.8, 11.6, 19.4, 25, and 48 Å-radius CdS nanoparticles [20]. Addition of judicious amounts of ethanol, 2-propanol, or acetone to aqueous dis-

Table 18.1. Preparations of CdS nanoparticles.

Method	Media/Stabilizer	Comments	References
Cluster synthesis	Aqueous/thiol derivatives	Structurally defined clusters with sizes ~ 1.0 – 1.6 nm in diameter were synthesized. NMR, X-ray single crystallographic characterization were carried out. Optical adsorption showed a strong exciton transition at about 290 nm.	[23–27]
Clay platelet compartmentalization	Aqueous/silicates nanoreactor	Size-quantized particles were prepared in nanophase reactors provided by binary liquids adsorbed at layered silicates. Optical absorption, XRD were used to characterize the particles.	[13, 28]
Hydrolysis in zeolites	Zeolite-X	CdS clusters were synthesized in zeolite-X through hydrolysis to form capped semiconductor nanoclusters. Optical properties were examined.	[29, 30]
Solid solution	Aqueous/silicates, silica	Growth of nanocrystals was studied in silicate glasses and in thin SiO_2 films in the initial stages of the phase separation of a solid solution, colloidal silica–CdS nanocomposites. Particles and clusters of semiconductor–metal sulfides were grown <i>in situ</i> in porous silica pillared layered phosphates.	[31–33]
Ultrasound	Aqueous/hexametaphosphate	Q-state CdS particles were generated by ultrasound at 20 kHz upon aqueous cadmium thiols.	[34]
Colloid synthesis, arrest precipitation, and size-selective partition	Aqueous or nonaqueous/small molecule stabilizers: aminocalixarene, TOPO, water-soluble thiols	Organically capped, highly monodisperse quantum-sized particles were made by colloidal route followed by size-selective precipitation. TEM, XRD, fluorescence emission, optical absorption characterization were carried out. Size-dependent oscillator strength, temperature shift of the excitonic transition energy, and reversible absorbency shift were observed.	[18–22, 35, 36]
Thermolysis	4-ethylpyridine	CdS and CdSe nanoparticles were synthesized by thermolysis of diethyldithio- or diethyldiseleno-carbamates of cadmium. Absorption spectra and TEM were used for characterization.	[37]

Electrodeposition

Aqueous electrolytes/Au single crystal on electrodes

Quantum dots were electrically deposited on Au(111) single-crystal domains coated on electrode. *Environ. Sci. Technol.* 34: 1000–1004 (2000). [38–42]

Thermolysis	4-ethylpyridine	energy, and reversible absorbency shift were observed. CdS and CdSe nanoparticles were synthesized by thermolysis of diethyldithio- or diethyldiseleno-carbamates of cadmium. Absorption spectra and TEM were used for characterization.	[37]
Electrodeposition	Aqueous electrolytes/Au single crystal on electrodes	Quantum dots were electrically deposited on Au(111) single-crystal domains coated on electrode. Epitaxial CdS and CdSe nanocrystals were characterized by TEM. Scanning tunneling microscopy of electrochemically grown CdS monolayers on Au(111) was done. Quantum size effects were investigated in the chemical solution deposition mechanisms of semiconductor films.	[38-42]
Polymer templates	Biopolymers, block polymers and porous polymers as compartments	II-VI semiconductor nanoparticles were synthesized by the reaction of a metal alkyl polymer adduct with hydrogen sulfide. Q-CdS clusters were stabilized by polynucleotides. Nanoparticles were also made within an ordered polypeptide matrix. Size control of nanoparticles in styrene-based random ionomers was studied. Spherical ionic microdomains were observed in styrene-based diblock ionomers. A Q-dot condensation polymer in chelate polymer microparticles was formed and polymer size dependence of the optical properties was studied. Amorphous polysilene quinoxanes were employed as a confinement matrix for quantum-sized particle growth. Nanoparticles were grown in porous polysilsequinoxanes.	[43-52]
Sol-gel technology	Borosilicate glass matrix, silica and silicate glass with and without inorganic salt additives	Oxidation of cadmium chalcogenide microcrystals, doped in silica glasses, prepared by the sol-gel process was investigated. Quantum confinement effects of CdS nanocrystals in a sodium borosilicate glass, prepared by the sol-gel process, were studied. Effect of heat and gases on the photoluminescence of CdS quantum dots confined in silicate glasses prepared by the sol-gel method was inspected. Optical properties of CdS nanocrystals dispersed in a sol-gel silica glass were studied.	[53-61]
Protein monolayer	CdS/channel protein	Nanosized CdS particles were formed within a channel protein monolayer on water.	[62]

Table 18.2. Preparations of CdSe nanoparticles.

Method	Media/Stabilizer	Comments	References
Electrodeposition	Aqueous electrolytes/ Au single crystal film coated on electrode	Epitaxial size control was achieved by mismatch tuning in electrodeposited Cd(Se, Te) quantum dots on Au (111). Electrodeposited quantum dots were found to be epitaxial. High-resolution TEM and electronic absorption spectra were employed to characterize the epitaxial nanocrystals.	[36, 39, 63]
Colloid synthesis, arrest precipitation, and size-selective precipitations	Aqueous or nonaqueous/ small molecule stabilizers: aminocalixarene, TOPO, and water-soluble thiols	Organically capped, highly monodisperse quantum-sized particles were made by colloidal route followed by size-selective precipitation. TEM, XRD, fluorescence emission, optical absorption characterization were carried out. Size-dependent oscillator strength, temperature shift of the excitonic transition energy, and reversible absorbency shift were observed.	[19, 20, 35]
Chemical solution deposition	Aqueous electrolytes	Quantum size effects were studied in chemical solution deposition mechanisms of semiconductor films.	[38]

Table 18.3. Preparations of ZnS and ZnSe nanoparticles.

Table 18.3. Preparations of ZnS and ZnSe nanoparticles.

Method	Media/Stabilizer	Comments	References
Colloid synthesis	Organic solvents/thiophenol, thioglycerol	Thiophenol-capped ZnS quantum dots 0.7–1.5 nm in diameter were prepared. XRD and optical absorption characterization were carried out. Thioglycerol-capped ZnS particles 1.2–1.5 nm in diameter were prepared. ESR spectra of the particles were compared with those of bulk ZnS.	[64]
Langmuir–Blodgett film	Organized surfactant LB films	Size-confined ZnS particles were synthesized in Langmuir–Blodgett films by the reaction of metal fatty acid with H ₂ S.	[65]
Organometallic block polymer	Lamella or spherical microphased polymers	ZnS clusters and zinc particles of about 3.0 nm in diameter were synthesized within microphase-separated domains of organometallic block copolymers. TEM and optical absorption characterization were carried out.	[66]
Polymer	Aqueous/polymer	ZnS and CdS particles were prepared by the reaction of a metal alkyl polymer adduct with H ₂ S in solution. TEM showed the particle sizes ranging from 2 to 5 nm in diameter. Absorption band edge changes were investigated by photoacoustic spectroscopy.	[45]
Polymer	Aqueous/polymer or chitosan	ZnS nanocrystals were prepared in a polymer matrix and in chitosan film. Electroluminescence was observed. ZnS thin films were grown by SILAR on poly(vinyl chloride) and polycarbonate substrates.	[67–69]
Clay platelet compartmentalization	Ethanol-cyclohexane/layered silicate or colloidal particles	Size-quantized CdS and ZnS particle dispersions were prepared in nanophase reactors provided by binary liquids adsorbed at layered silicates and at colloidal silica particles. XRD, rheological, and calorimetric measurements were performed to characterize the dispersions.	[13, 28]
MOCVD	Vacuum	Intrazeolite topotactic MOCVD was used for three-dimensional structure-controlled synthesis of II–VI nanoclusters.	[70]
Sol-gel processing	Aqueous	Electroluminescent ZnS devices were produced by sol-gel processing. Sol-gel-derived ZnSe crystallites were prepared in glass films and optical properties were studied.	[71, 72]

Table 18.4. Preparations of ZnO nanoparticles.

Method	Media/Stabilizer	Comments	References
Colloid synthesis	Aqueous, ethanol, and 2-propanol	Transparent sol was prepared in water and ethanol or 2-propanol. Fluorescence spectra show that adsorbed electron relays are necessary to transport electrons from conduction band to deep traps.	[73]
Sol-gel technology	Aqueous/conducting glass	Transparent nanocrystalline ZnO film was prepared by sol-gel techniques. Visible-light sensitization by <i>cis</i> -bis(thiocyanato) bis(2,2'-bipyridyl-4,4'-dicarboxylato) ruthenium(II) on the film was shown to have high light-to-current conversion efficiency.	[74]
Polymer matrix	Aqueous/polymer	ZnO nanoparticles were synthesized with capsulation of polymer. Steady and time-resolved fluorescence, absorption spectroscopy were used to characterize the particles.	[75]
Electrodeposition	Aqueous/electrode	Cathodic electrodeposition was accomplished from aqueous solution to form dense or open-structured ZnO films.	[76]
Sublimation	Vacuum	Quantum size effects in zinc oxide nanoclusters were synthesized by reactive sublimation. TEM, XRD, and photoacoustic FTIR data were obtained.	[77]
Laser vaporization	Vacuum	Metal oxide nanoparticles were synthesized by using laser vaporization/condensation in a diffusion cloud chamber.	[78]

Table 18.5. Preparations of PbS nanoparticles.

Table 18.5. Preparations of PbS nanoparticles.

Method	Media/Stabilizer	Comments	References
Polymer	Aqueous or organic solvents/polymer	Metal sulfide nanoparticles were prepared by the reaction of soluble metal alkyls and polymers containing pyridyl groups with H ₂ S. The particles were observed by TEM to be evenly distributed in the polymer matrix.	[79]
Polymer	Benzene/Pb-containing polymer film	PbS nanoclusters were synthesized within microphase-separated diblock copolymer films and within block copolymer nanoreactors. TEM, XRD, and electronic absorption were employed to characterize the particles embedded in the films.	[70, 80, 81]
Langmuir-Blodgett film	Fatty acid or amphiphilic polymers in ordered films	Size-confined metal sulfides were synthesized in Langmuir-Blodgett films. Control of distance and size of the nanoparticles was achieved by organic matrices in the LB films.	[82, 83]
Monolayer	Surfactant monolayer on water surfaces	Morphology control was accomplished for epitaxially grown PbS nanocrystallites under mixed surfactant monolayers. Morphology-dependent spectroelectrochemical behavior of the nanoparticulate films was studied on conducting glass electrode in electrochemical cell.	[84, 85]
Surfactant mesophase	Aqueous/AOT	Quantum-sized PbS particles were prepared in surfactant-based complex fluid media and in bicontinuous cubic phase of AOT. Structural and morphological characterization by TEM, small-angle X-ray scattering were carried out.	[86, 87]
Sol-gel processing	Aqueous/silicon methoxide, boron ethoxide	PbS quantum dot materials were prepared by the sol-gel process using Pb-doped gel of silicon methoxide or boron ethoxide and lead acetate followed by sintering.	[88]

Table 18.6. Preparations of GaAs and other III-V nanoparticles.

Method	Media/Stabilizer	Comments	References
Colloid synthesis	Decane/methylsilane	3 nm GaAs crystallites were prepared by refluxing GaCl ₃ with As(SiMe ₃) ₃ at 180°C. The particle growth was controlled by autoclaving. Electronic absorption spectra were studied.	[89]
Colloid synthesis	Organic solvents/ monoglyme or diglyme	Nanocrystalline GaAs and GaP were synthesized in organic solvents by a route of <i>in situ</i> formation of particles followed by metathetical reaction with coordinate solvents. UV, TEM, XRD, and elemental analysis were used to characterize the nanoparticles.	[90]
Colloid synthesis	Aromatic solvents/ chelating agents	5 nm-diameter GaAs nanoparticles were prepared via metathetical reaction of GaCl ₃ with chelating agents bearing As(III). XRD, XPS, NMR, FTIR, high-resolution TEM characterization were carried out.	[91]
Colloid synthesis	Triethylene glycol ether/ methylsilyl	GaAs quantum dots were synthesized by the reaction of gallium acetylacetonate with trimethylsilylarsine at 216 K. The particles were characterized by XRD, XPS, UV, and elemental analysis. Transient pump-probe spectroscopy was used to examine charge carrier transport.	[92]
Colloid synthesis	Organic solvent/TOPO	2.6 nm InP nanocrystals were synthesized by reacting chlorindium oxalate complex with P(SiMe ₃) ₃ at 270°C. The nanoparticles were characterized by TEM and optical absorption.	[93]
Colloid synthesis	Triglyme	Size-quantized GaAs nanocrystals 1.5–9.0 nm in diameter were prepared by wet process. Photoinduced reduction of methyl viologen on the particles was investigated.	[94]
			[95–97]

pensions of colloidal CdS resulted in the preferential precipitation of the larger nanoparticles, while the smaller ones remained in the supernatant. Centrifugation permitted the separation of the precipitate and the supernatant and thus it provided the means for isolating CdS nanoparticles in narrow size distributions.

- Structurally defined clusters (containing 15–45 molecules) of semiconductors [23–27] can now be chemically synthesized and crystallized in a superlattice structure.

The recently reported preparations of $\text{Cd}_{32}\text{S}_{14}(\text{SC}_6\text{H}_5)_{36}\text{DMF}_4$ [26] and $\text{Cd}_{17}\text{S}_4(\text{SCH}_2\text{CH}_2\text{OH})_{36}$ [27] clusters illustrate the current activities in this area. The structure of the yellow cubic crystalline $\text{Cd}_{32}\text{S}_{14}(\text{SC}_6\text{H}_5)_{36}\text{DMF}_4$ was determined to consist of a 12 Å-diameter spherical 82-atom CdS core with dangling surface bonds terminating in hexagonal (wurtzitelike) CdS units at the four tetrahedral corners [26]. Two clusters of $\text{Cd}_{17}\text{S}_4(\text{SCH}_2\text{CH}_2\text{OH})_{36}$ were observed to assemble to an interlaced diamondlike superlattice [27]. Importantly, both of these clusters remained intact upon dissolving them in dipolar aprotic solvents, and their absorption and emission spectra, both in the solid state and in colloidal dispersions, indicated size quantization.

- Nanoparticles can be generated *in situ* in (or at) such membrane mimetic systems [5, 31] as aqueous and reversed micelles, surfactant vesicles, proteins, monolayers, Langmuir–Blodgett (LB) films, bilayer lipid membranes (BLMs), polymers, polyelectrolytes, synthetic membranes, silicates (organoclay complexes or pillared silicates, for examples), and porous glass.

Aqueous micellar cobalt and iron(II) dodecyl sulfate have been employed for the preparation of nanosized cobalt and iron magnetic particles [98]. The size of the particles was controlled by the surfactant concentration. The average size of the particles, determined by transmission electron microscopy and by comparison with simulated Langevin curves, varied from 2 to 5 nm, with 30–35% polydispersity in the size distribution and thus they were superparamagnetic. The saturation magnetization was found to decrease and the surface anisotropy to increase with an increase in size of the nanoparticles.

Reversed micelles are surfactant-entrapped water pools in an organic solvent, and the water-to-surfactant molar ratio determines the size of the water pool. Aerosol-OT (sodium dialkylsulfosuccinate) has been the favored surfactant for reversed micelle formation since it can solubilize up to 50 moles of water per mole of surfactant and since its properties in organic solvents are well understood [99]. Sizes of nanoparticles, generated *in situ* in reversed micelles, have been controlled by the judicious selection of water-to-surfactant ratios, by using functionalized surfactant (replacing the sodium ion by the copper ion in Aerosol-OT for copper particle formation, for example [100, 101]) and by arresting the growth of nanoparticles by capping them by a nucleophilic reagent (thiophenol, for example [20, 102]).

Nanoparticle precursor ions can be selectively attracted to, and hence nanoparticles can be grown at, the inner or the outer surfaces of surfactant vesicles [103]. This arrangement has permitted the demonstration of vectorial photoelectron transfer in surfactant vesicles [103]. Similarly, nanoparticles have been prepared at one or both sides of bilayer lipid membranes [102].

Hydrophilic cavities in channel proteins provide a suitably confined space for nanoparticle generation. Cadmium and zinc sulfides have been formed, for example, within the cavity of a channel protein by a simple process in which a closely packed monolayer of the channel protein is formed on a neutral subphase, transported to a cadmium-chloride-containing subphase, transferred to a slide by Langmuir-Blodgett transfer, and exposed to hydrogen sulfide [62]. The size of the cluster formed is limited by the small number of ions capable of assimilation into the channel and, because each group of ions is compartmentalized, there is no possibility of spontaneous aggregation to produce macroscopic particulates inside of the protein channel.

Semiconducting, metallic, and magnetic nanoparticulate films have been grown under monolayers whose aqueous subphase contained the appropriate precursor ions (Cd^{2+} , Ag^+ , $\text{Fe}^{2+}/\text{Fe}^{3+}$, for example) upon exposure to gaseous precursors (H_2S , formaldehyde, for example) [5, 105]. Silver ions, attached to negatively charged monolayers have also been reduced by *in situ* electrolysis [6, 105].

Advantage has also been taken of the hydrophilic interlayers of Langmuir-Blodgett films to incorporate or *in situ* generate nanoparticles [106–109]. Formation of CdS nanoparticles in cadmium arachidate Langmuir-Blodgett films has been monitored by an electrochemical quartz crystal microbalance (EQCM) and absorption spectrophotometry [106]. The formation of CdS nanoparticles was consistent with that expected for the quantitative conversion of Cd^{2+} ions in the films to CdS and the corresponding conversion of CdAr to arachidic acid. Subsequent reexposure of the film to H_2S increased the mole fraction of CdS in the film. Indeed, exposing a cadmium stearate Langmuir-Blodgett (LB) film to H_2S , then immersion in aqueous CdCl_2 was found to regenerate the cadmium stearate multilayer without the escape of CdS and the repetition of sulfidation-intercalation cycles allowed the size-quantized CdS to grow in a stepwise fashion within the hydrophilic interlayers [106]. This approach opens the door to the formation of nanoparticles in controllable thickness.

Polar liquids selectively adsorbed at solid interfaces from binary apolar-polar liquids have been shown to provide a suitable nanoreactor for the generation of nanoparticles [28]. Precise information on the volume of the nanoreactor, in a given system, can be obtained by the determination of excess adsorption isotherms. Thus, for example, in silica particle dispersions in ethanol-cyclohexane and in methanol-cyclohexane binary mixtures 0.5–5.0 nm-thick alcohol-rich adsorption layers have been shown to form at the silica-particle interface. This alcohol nanolayer has been used for the generation of controlled-sized CdS and ZnS particles [28].

A large variety of different nanoparticles have been prepared in the cavities provided by porous glasses, membranes, and zeolites [30, 74]. The current trend is to alter the pore sizes and chemical composition by derivatization or chemical synthesis.

- Using suitable templates it is possible to control the shapes of incipient nanoparticles and to grow them epitaxially [101].

The shape of the template has been shown to profoundly influence the shape of the nanoparticles grown thereon (or therein). Evidence has been reported, for example, for the formation of spherical and cylindrical copper nanoparticles in spherical and cylindrical reversed micelles [101].

Monolayers spread on aqueous solution surfaces have been shown to provide suitable templates for oriented crystallization of nanoparticles [85, 109–111]. Lead sulfide (PbS) particulate films composed of highly oriented, equilateral triangular crystals have been generated *in situ* by the exposure of arachidic acid (AA) monolayer-coated aqueous lead nitrate solutions to hydrogen sulfide. The AA-coated PbS particulate films, at different stages in their growth, were transferred to solid substrates and characterized by transmission electron microscopy (TEM), atomic force microscopy (AFM), and electron diffraction measurements. Each individual crystal had its (111) plane parallel and its (112), (121), and (211) plane perpendicular (arranged in threefold symmetry at 120° angles) to the AA monolayer surface. This epitaxial growth has been rationalized in terms of an almost perfect fit between the (111) plane of the cubic crystalline PbS and the (100) plane of the hexagonally close-packed AA monolayer [110]. Interestingly electrical and spectroelectrical properties of epitaxially grown PbS nanocrystals were found to be morphology dependent [89]. CdS [111, 112] and CdSe [113] have also been grown epitaxially under Langmuir monolayers [111].

- Chemical and colloid chemical approaches can be extended to many other nanoparticle preparations.

It is not unfair to say that only our lack of imagination and ingenuity limits us in preparing nanoparticles of any composition, size, and shape by suitable chemical means. Indeed, new and innovative preparations of metallic, semiconducting, magnetic, and ferroelectric nanoparticles appear with ever increasing frequency.

The desirable properties and potential applications (components of diode lasers and nonlinear electro-optical devices, for example) of gallium arsenide, indium arsenide, gallium phosphide, and indium phosphide quantum wells and superlattices prompted the ever increasing effort to design novel preparations of these nanoparticles. Indeed, several viable gallium arsenide [89, 94–96], gallium phosphide [90, 91], indium arsenide [97], and indium phosphide [93] preparations have been reported. Equally important is the ongoing intensive effort to prepare surface-oxidized silicon [114–116] nanoparticles that have unique photoluminescence properties.

18.2.3 Preparation of Composite Nanoparticles, Nanoparticle Arrays, and Nanostructured Films

Recent activities are summarized in Table 18.7, some of which are highlighted below.

Table 18.7. Preparations of composite nanoparticles.

Method	Particles Components	Comments	References
Heterosupramolecular synthesis	CdSe, diamine	Homodimers of CdSe nanocrystals were synthesized and characterized by TEM and electrophoresis.	[119]
Heterosupramolecular synthesis	TiO ₂ , cyanopyridino organics TiO ₂ , pyridinium organics	Polyviologen-modified TiO ₂ prepared by photocatalytic polymerization of bis(4-cyano-1-pyridinio)-p-xylene dibromide. Photoinduced electron transfer processes were observed in organized redox-functionalized bipyridinium-polyethylenimine-TiO ₂ colloids and particulate assemblies.	[122] [123]
Solid solution	CdSe, molecular bridge	CdSe nanocrystallite networks were built with molecular connectors.	[124]
Electrospray MOCVD	CdSe/ZnSe	Luminescent thin-film CdSe/ZnSe quantum dot composites were synthesized by electrospray MOCVD using CdSe quantum dots passivated with an overlayer of ZnSe. The films were characterized by XRD and luminescence spectroscopy.	[125]
Polymer	Mn/ZnS	Mn-doped ZnS nanocrystals were precipitated with a poly(ethylene oxide) matrix. Photoluminescence excitation was employed to study the dopant effect on bandgap and the size quantization.	[117]
Colloid synthesis	CdS, HgS	A quantum dot quantum well CdS/HgS/CdS was combined in aqueous sol synthesis. TEM and fluorescence decay data were obtained. Chemistry and photophysics of mixed layered CdS/HgS colloids were investigated.	[126, 127]
Colloid synthesis	CdS, CdSe	Coupled composite CdS-CdSe and core-shell types of (CdS/CdSe and (CdSe)/CdS nanoparticles were synthesized in aqueous sol form. TEM and optical absorption were used to characterize the composites. Luminescence spectral showed charge carrier transfer between CdS and CdSe moieties.	[118]
Colloid synthesis	CdS, SiO ₂	Monodisperse colloidal silica CdS nanocomposites were prepared by controlled hydrolysis of tetraethyl orthosilicate. Tailored morphology was observed by TEM and SEM. XRD and light-scattering characterization were carried out to show the size of CdS to be 2.5 nm in diameter.	[33]
Colloid synthesis	TiO ₂ , SnO ₂	Capped TiO ₂ -capped SnO ₂ nanocrystallites were prepared in colloid dispersion. Photoelectrochemical behavior of the composite particles was studied.	[128]

Colloid synthesis	CdS, SiO ₂	Monodisperse colloidal silica CdS nanocomposites were prepared by controlled hydrolysis of tetraethyl orthosilicate. Tailored morphology was observed by TEM and SEM. XRD and light-scattering characterization were carried out to show the size of CdS to be 2.5 nm in diameter. [33]
Colloid synthesis	TiO ₂ , SnO ₂	Capped TiO ₂ -capped SnO ₂ nanocrystallites were prepared in colloid dispersion. Photoelectrochemical behavior of the composite particles was studied. [128]
Nanoporous matrix	CdS, ZnS	Nanocomposite systems were grown <i>in situ</i> in porous silica-pillared layered phosphates. [129]
Solid solution	CdS, CdSe	CdS _x Se _{1-x} nanocrystals were grown in silicate glass. Their structural and interfacial properties were studied by high-resolution TEM and optical absorption. [130]
Solid solution	CdS, metals	Growth kinetics and quantum size effects of CdS nanocrystallites were examined in glasses. Metals were coated on semiconductor particles embedded in glass. [131, 132]
Xerogel	Cr, CdS	Nanosized Cr clusters and intimate mixtures of Cr/CdS phases were synthesized in a porous hybrid xerogel by an internal doping method. New procedures were analyzed for the preparation of CdS and heterogeneous Cr/CdS phases in hybrid xerogel matrices' pore structure. [133]
Photoreduction	Rh, TiO ₂ , SiO ₂	Homogeneous Rh particles were generated by photoreduction of Rh(III) on TiO ₂ colloids grafted on SiO ₂ . [134]
Evaporation of metal in reaction gas	TiO ₂ , SiO ₂	Quantum-sized TiO ₂ supported on silica were prepared. UV, LEES, XPS, and REELS were used to characterize the composites. Spectroscopic features were used to examine the influence of size and support on photoemission of the composites. [135]
Porous matrix	TiO ₂ , PbS, Ag ₂ S	Porous TiO ₂ was sensitized by PbS quantum dots. Photoconduction properties were studied. Particle size and pH effects on the sensitization of nanoporous TiO ₂ electrodes by Q-sized Ag ₂ S were investigated. [136, 137]
Colloid synthesis	TiO ₂ , Fe, Mo, Ru, Os, Re, V	Role of metal ion dopants in quantum-sized TiO ₂ was studied and correlation between photoreactivity and charge carrier recombination dynamics was established. [138, 139]
Blending	CdSe, polymer	Electroluminescence was observed for CdSe quantum dot polymer composites. [140]
Sol-gel processing	TiO ₂ , 4-(dimethylamino)-4'-nitrostilbene, 4-(2-(4-hydroxyphenyl) ethyl)-N-methylpyridium	TiO ₂ film doped with organic compounds was made by two-dimensionally poled sol-gel processing for nonlinear optical activity. [141]
Sol-gel processing	TiO ₂ , SiO ₂	
Sol-gel processing	RuO ₂ , TiO ₂	Selective epoxidation of α -isophorone was achieved with mesoporous titania-silica aerogels and tert-butyl hydroperoxide. [142]
		Ultrafine RuO ₂ -TiO ₂ binary oxide particles were prepared by a sol-gel process. [143]

- Composite and core-shell types nanoparticles can now be routinely prepared.

Depending on the method of preparation, it is quite possible to vary the composition of composite nanoparticles. H_2S exposure of a monolayer floating on a mixture of aqueous cadmium nitrate and zinc nitrate solutions, for example, leads to the formation of composite $\text{CdS}_x\text{ZnS}_{1-x}$ nanoparticulate films [105]. The ratio of CdS to ZnS in the mixed nanoparticulate films could be varied by changing the ratio of the precursor ions in the subphase. A similar approach was used in forming mixed $\text{MnS}_x\text{ZnS}_{1-x}$ nanoparticulates in reversed micelles [117].

Sequential generation of two (or more) different nanoparticles results in the formation of core-shell-type structures [105, 118]. By paying careful attention to the different parameters (the order, the amount, and the rate of precursor introduction) it is quite feasible to achieve a fine level of thickness control of the different layers (core and shell, for example). Due attention has to be paid, however, to the solubility products of the nanoparticles. For example, the larger solubility product of ZnS than PbS permits the replacement of lead ions by zinc ions upon the immersion of PbS nanoparticles into an aqueous zinc ion solution. Conversely, because of their solubility products, lead ions cannot replace zinc ions in ZnS. Introduction of zinc ions into PbS is tantamount, of course, to doping. The extent of doping can be controlled, at least to some extent, by varying the time of exposure of the semiconductor nanoparticles to the dopant ions.

Sandwich layers of PbS and ZnS nanoparticulate films have been prepared under monolayers [105]. The method involved the following steps: (i) formation of the PbS nanoparticulate film by exposing a monolayer (floating on aqueous $\text{Pb}(\text{NO}_3)_2$ subphase) to H_2S , (ii) exchanging the aqueous $\text{Pb}(\text{NO}_3)_2$ subphase to aqueous $\text{Zn}(\text{NO}_3)_2$ subphase without perturbing the monolayer-supported PbS nanoparticulate films, and (iii) formation of the ZnS nanoparticulate film by exposing a monolayer-supported PbS (floating on aqueous $\text{Zn}(\text{NO}_3)_2$ subphase) to H_2S .

Core-shell-type (CdS)CdSe (or (CdSe)CdS) nanoparticles have been prepared by the sequential introduction of different amounts of H_2S and H_2Se (or H_2Se and H_2S) into aqueous $\text{Cd}(\text{ClO}_4)_2$ solutions containing $(\text{NaPO}_3)_6$ [118]. Conditions in these experiments were adjusted (by adding excess cadmium and hydroxide ions) for the maximization of excitonic fluorescence. Two emission bands were observed in the coupled and in the core-shell-type mixed semiconductor nanoparticles. The first one, centered around 470 nm, was attributed to the $1s(e)-1s(h)$ excitonic emission of CdS. The second, centered around 560 nm, was proposed to arise from charge transfer of CdS to core-shell-type (CdS)CdSe (or (CdSe)CdS) nanoparticles [118].

- Chemists have learned to treat nanoparticles as large macromolecules and to link them, by electrostatic interactions or covalent bonds, into heterostructured supramolecules, two-dimensional arrays, or three-dimensional networks.

The recognition that nanoparticles can be derivatized and treated like any other molecule is a major development in our quest for the full exploitation of chemistry

for advanced materials synthesis. The following examples all illustrate our accomplishments in reacting and assembling nanoparticles.

Two thiol-capped cadmium selenide nanocrystals have been covalently linked by the addition of a bis(acyl hydrazine) derivative to give a stable homodimeric CdSe product [119]. CdS and TiO_2 nanoparticles have been bridged [120]. Phosphonated polypyridyl ligands have been used to anchor transition metal complexes to titanium dioxide nanoparticulate films [121]. Gold nanocrystals, each encapsulated by a monolayer of alkyl thiol molecules, have been cast from a colloidal solution onto a flat substrate to form a close-packed monoparticulate layer [144]. Adjacent clusters have then been covalently linked by aryl dithiols or aryl di-isonitriles, which displaced the alkyl thiol molecules in the monolayer and formed a two-dimensional superlattice of gold nanoparticles that exhibited nonlinear Coulomb-charging behavior when placed in the gap between two gold contacts [144]. An even simpler method of assembly of gold nanoparticle superlattices has been accomplished by an acid-facilitated phase transfer (from an aqueous dispersion to toluene) of thiol-derivatized Au, Pt, and Ag nanoparticles [145].

Of particular significance is the employment of DNA for the reversible assembly of nanoparticles into desired three-dimensional networks [146, 147]. The method involves the attachment of single-stranded DNA oligonucleotides of defined length and sequence to nanoparticles via thiol linkages and the assembling of the desired structures by Watson-Crick-type complementary base pairing. Thermal denaturation results in the disassembly of the supramolecular structure formed. The advantage of this approach is its versatility and diversity, which, at least in principle, permit the manufacturing of any tailor-made advanced nanoparticle-based materials by well-established biochemical protocols.

Self-assembly of alternative nanolayers of oppositely charged polyelectrolytes and nanoparticles provides a convenient means for the preparation of two-dimensional arrays and three-dimensional networks of simple and composite nanoparticles. Self-assembly of macromolecular species into larger units is well established in nature, of course. It is only recently that chemists have been able to mimic this process. They have layer-by-layer self-assembled oppositely charged polyelectrolytes and polyelectrolyte-nanoparticle films [148]. The layer-by-layer self-assembly of polyelectrolytes and nanoparticles onto substrates is deceptively simple. A well-cleaned substrate is primed by adsorbing a layer of surfactant or polyelectrolyte onto its surface. The primed substrate is then immersed into a dilute aqueous solution of a cationic polyelectrolyte, for a time optimized for adsorption of a monolayer, rinsed, and dried. The next step is the immersion of the polyelectrolyte monolayer-covered substrate into a dilute dispersion of surfactant-coated negatively charged nanoparticles, also for a time optimized for adsorption of a monoparticulate layer, rinsing, and drying. These operations complete the self-assembly of a polyelectrolyte monolayer-monoparticulate layer of semiconductor nanoparticle sandwich unit onto the primed substrate. Subsequent sandwich units are deposited analogously. Alternating polyelectrolyte monolayers and CdS [148], PbS [149], TiO_2 [149], BaTiO_3 [149], lead-zirconate-titanate, PZT [150], and Au [151] monoparticulate layer sandwich units have been prepared this way.

The method of self-assembly is extremely versatile. Sandwich units can be layered in any order for a variety of different nanoparticles. Furthermore, elimination of the polyelectrolyte layers by burning leads to ultrathin films in which the nanoparticles are arranged in a three-dimensional network with controllable interparticle distances. Such films are, of course, extremely useful for many practical applications. For example, the self-assembly of monodisperse gold and silver colloid particles into monolayers on polymer-coated substrates yields macroscopic surfaces that are highly active for surface-enhanced Raman scattering (SERS) [151] and optically nonlinear materials [152].

Spreading surfactant-stabilized nanoparticles on aqueous solutions in a Langmuir trough and transferring them to solid substrates by the Langmuir-Blodgett technique provide an alternative approach to superlattice construction [153, 154]. The technique can be regarded as analogous to monolayer formation from simple surfactants. There are many intrinsic benefits to this method. That the particles are prepared prior to their incorporation into the films enables their dimensions and physical properties and the particle size distribution to be precisely controlled. Spreading the particles in a Langmuir trough provides a means for defining the interparticle distances and facilitates subsequent transfer of the particulate films to a wide range of solid substrates by using standard Langmuir-Blodgett (LB) techniques. This may be contrasted with deposition techniques, where the quality of the film is highly dependent on the solid substrate itself. Thus, in essence, this method is highly versatile, facilitating film construction from a diverse range of materials and substrates; it is also extremely simple experimentally. Additionally, it is quite possible to affect the layer-by-layer transfer of different nanoparticles and thus form a composite three-dimensional structure.

Surfactant-coated cadmium sulfide [153, 154], TiO_2 [155], the magnetic iron oxide magnetite Fe_3O_4 [156], ferroelectric barium titanate [150], lead zirconium titanate [157], Pt [158], Pd [158], and Ag [159, 160] nanoparticles have been prepared to date in our laboratories by this Langmuir monolayer LB-film technique. In all cases, particulate films were spread on water in a Langmuir trough by dispersing solution aliquots from a Hamilton syringe. Physical properties of the monoparticulate films were characterized, *in situ*, on the water surface and subsequently transferred to solid substrates, by using a range of physical techniques. The structures of the films on the water subphase were examined on the micrometer scale by Brewster-angle microscopy (BAM) and at higher magnifications by transmission electron microscopy (TEM). Absorption spectroscopy and steady state fluorescence spectroscopy were applied where appropriate, and reflectivity measurements permitted the estimation of film thicknesses on water surfaces. Standard techniques were applied for the LB transfer. The surfactant coating of the nanoparticles can, of course, be burned off to produce the desired ultrathin nanoparticulate film.

The construction of nanoparticle arrays and nanostructured films is summarized in Table 18.8.

Table 18.8. Fabrications of nanoparticle arrays and nanostructured films.

Method	Particles/Substrates	Comments	References
Electrodeposition Monolayer	TiO ₂ /electrode TiO ₂ /PbS	Nanocrystalline TiO ₂ thin films were prepared by cathodic electrodeposition. Monolayers of TiO ₂ /PbS coupled nanoparticles were formed by electrostatic attraction. TEM, XPS, and absorption spectroscopy were used to characterize the films.	[161] [162]
Langmuir-Blodgett deposition	CdSe, CdS, TiO ₂ /glass, TEM grids, metal electrode	Langmuir-Blodgett films of size-selected CdSe nanocrystallites were prepared. TEM, absorption and emission spectroscopy were used to characterize the film. LB films were made from fluorescence-activated, surfactant-capped, size-selected CdS nanoparticles. AFM, STM were employed to image the surfaces. Monoparticle layer and layers of size-quantized CdS clusters were fabricated by LB techniques. Monoparticle layers of TiO ₂ nanocrystallites were deposited with controllable interparticle distances. CdS clusters were generated in an organic bilayer template to form an organic-inorganic superlattice structure.	[21, 153, 154, 158-160]
Organized bilayer	CdS/bilayer cast film	Thin and superthin photoconductive CdSe films were deposited on substrate at room temperature.	[104]
Deposition	CdSe/solid supports	Self-assemblies of semiconductor nanocrystals were surveyed on thiol-functionalized Au surfaces. Self-assembling multilayer structures were studied by quartz crystal microgravimetry.	[166]
Self-assembly	Au, CdS	Light-emitting diodes were made from CdSe nanocrystals and a semiconducting polymer.	[167, 168]
Self-assembly	CdSe/thiol organics on ITO electrode CdS/porous film	Quantum-sized CdS particles were assembled to form a regularly nanostructured porous film.	[170]
Surfactant liquid crystal	WO ₃ , Sb ₂ O ₃ /surfactant organized layers	Organic molecules with inorganic molecular species were organized into nanocomposite biphasic arrays.	[171]
Solution decomposition epitaxy	CdS/silicon wafer	CdS nanostructured films were deposited by decomposition of thiourea in basic solution.	[172]
Atomic layer epitaxy	TiO ₂	Titanium isopropoxide was used as a precursor in atomic layer epitaxy of TiO ₂ thin films. Atomic layer epitaxy growth of TiO ₂ thin films from titanium ethoxide.	[167] [168, 169]

Table 18.8. (cont.)

Method	Particles/Substrates	Comments	References
Aggregation	CdS	Ultrathin semiconductor films were formed by CdS nanostructure aggregation.	[170]
Chemical solution deposition	CdO, CdS, ZnO, ZnS	Nanoclusters were embedded in siliceous faujasite.	[171]
	CdS, TiO ₂	CdS films were deposited by decomposition of thiourea in basic solutions. TiO ₂ thin films were prepared from aqueous solution.	[172, 173]
Chemical solution deposition	ZnO	Transparent and conductive ZnO thin films were prepared by applying a solution of zinc alkoxide. Spectroelectrochemical investigations of nanocrystalline ZnO films.	[174, 175]
Chemical solution deposition	CdS	CdS thin films comprising nanoparticles were prepared by a solution growth technique.	[176]
Electrochemistry	TiO ₂ /polymer mold	TiO ₂ nanotube array was formed by electrochemical deposition in a polymer mold.	[177]
Electrochemistry	TiO ₂	Photoelectrochemical doping of TiO ₂ particles and the effect of charge carrier density on the photocatalytic activity of microporous semiconductor electrode films were studied.	[178]
Adsorption	TiO ₂	Photochemical quartz crystal microbalance was used to study the nanocrystalline TiO ₂ semiconductor-electrode-water interfaces.	[179]
		Simultaneous photoaccumulations of electrons and protons were investigated.	
Colloid synthesis	SnO ₂ /TiO ₂	Photoelectrochemical behavior of SnO ₂ /TiO ₂ composite systems and its role in photocatalytic degradation of a textile azo dye were investigated.	[128]
Sol-gel technology Nanochannel glass	TiO ₂	TiO ₂ ultrathin films were prepared by two-dimensional sol-gel process.	[180]
	GaAs, InAs/ nanochannel glass	GaAs and InAs nanowires, in the form of 3–15 nm crystallites, were prepared by reaction of organogallium or organoindium with arsine in porous nanochannel glass.	
Chemical beam epitaxy	GaAs film	Nanostructured GaAs films were grown using tris(di-ter-butylarsino)gallane as single source precursor in chemical beam epitaxy.	[182]

18.3 Properties of Bulk Semiconductors and Semiconductor Nanoparticles Compared and Contrasted

The structural, optical, and electronic properties of intrinsic bulk CdS, CdSe, ZnS, ZnSe, PbS, TiO₂, GaAs, Ge, and Si semiconductors are summarized in Table 18.9. These properties are not expected to change for a given semiconductor with changes in size or shape. In contrast, both the optical and the electronic behaviors of semiconductor nanoparticles are distinctly size dependent. In fact, the major advantage of using semiconductor nanoparticles is that the optoelectronic properties can be tailored quite simply by size alteration without changing the chemical composition of the material. This behavior spectacularly manifests itself in size-dependent color changes. The black bulk PbS can be made, for example, red, yellow, and even colorless if prepared as progressively smaller- and smaller-diameter nanoparticles. The practical relevance of size-quantized semiconductor particles is that upon photoexcitation the undesirable electron-hole recombination diminishes since the smaller the particle the larger the surface-area-to-volume ratio, and hence the ease of electron transfer to surface-bound acceptors or donors. That the size quantization decreases the absorption edge and hence increases the required excitation energy is another matter.

A related, and often forgotten, issue is that for size-quantized particles morphological changes often influence electrical and optoelectrical behavior. For example, the differences in morphology between equilateral-triangular PbS (PbS-I), right-angle-triangular PbS (PbS-II), both epitaxially grown under monolayers (prepared from AA:ODA = 1:0 and AA:ODA = 1:1), and disk-shaped PbS (PbS-III, non-epitaxially grown under monolayers, prepared from hexadecylphosphonic acid), manifested themselves in different spectroelectrochemical behavior [85]. Specifically, marked differences were observed in the potential-dependent absorption spectra of PbS-I, PbS-II, and PbS-III. Biasing the epitaxially grown PbS-I and PbS-II nanoparticulate films to negative potentials (from 0.5 V to -1.1 V) increased the intensity of absorption in the ultraviolet region. In contrast, no change in the absorption at wavelengths longer than 700 nm was observed in the non-epitaxially grown PbS nanoparticulate film on changing the potential from 0 to -1.5 V. Absorption spectra of the optically transparent conductive glass (i.e., the control) remained unaltered upon biasing the potential between +0.5 and -1.5 V. The near-infrared absorption is likely to correspond to the spectrum of trapped charge carriers. Increase of this absorption resulted from the accumulation of trapped conduction band electrons at negative bias potentials in PbS-I and PbS-II. Indeed, absorbances for PbS-II at 750 nm were found to decrease with increasing applied positive potential linearly to -0.6 V, after which they remained unaltered. The point of inflection, -0.50 ± 0.05 V, may be taken to correspond to the flat-band potential, V_{fb} , of the PbS-II nanoparticulate film [85]. Similarly, marked differences in capacitance vs. potential and photocurrent curves were observed between PS-I, PS-II, and PS-III [85]. Dependence of the absorbance on the applied potential, as well as the observed photocurrent and voltage-dependent capacitances, reflected a

by reaction of organogallium or organoindium with arsine in porous
nanochannel glass. [182]
Nanostructured GaAs films were grown using tris(di-ter-butylarsino)gallane as
single source precursor in chemical beam epitaxy.
nanochannel glass
GaAs film
Chemical beam
epitaxy

Table 18.9. Solid state physical properties of selected semiconductors.¹

Property	CdS	CdSe	ZnS	ZnSe	PbS
Lattice parameters (Å)	Hexagonal: $a = 4.136, c = 6.714$	Hexagonal: $a = 4.299, c = 7.011$	Hexagonal: $a = 3.8226, c = 6.2605$	Hexagonal: $a = 3.996, c = 6.540$	Orthorhombic: $a = 11.28, b = 3.98, c = 4.21$
Density (g cm^{-3})	Zincblende: $a = 5.818$ Rocksalt: $a = 5.42$	Zincblende: $a = 6.052$ Rocksalt: $a = 5.49$	Zincblende: $a = 5.4102$	Zincblende: $a = 5.6676$	Rocksalt: $a = 5.936$
Melting point (K)	4.82 1750	5.81 1514	4.075 Sublime before melting	5.266 1793	7.597 1383
Bandgap (eV)	~ 2.554 – 2.599	~ 1.751 – 1.771	~ 3.9107 – 3.9407 (hex.) ~ 3.68 – 3.74 (zinc.)	~ 2.70 – 2.82 (295 K)	0.286 (4.2 K) 0.42 (300 K)
Optical absorption edge (nm)	481–489	697–704	314–317 (hex.) 331–336 (zinc.)	~ 439 – 459	2951 (300 K)
Exciton energies (eV)	~ 2.5517 – 2.5528	~ 1.8249 – 1.8266	~ 3.698 – 3.801 (zinc., 273 K) ~ 3.8715 – 3.8932 (hex., 77 K)	~ 2.793 – 2.803	
g factor	1.789, 1.774, 1.75, 1.23, 1.8, 0.7	$g_{\text{eff}} = 0.6, g_{\text{eL}} = 0.51,$ $g_{\text{vL}} = 1.41$	$g_{\text{c}} = 1.8846,$ $g_{\text{v}} = 0.93,$ $m_{\text{n}} = 0.34$	$g_{\text{c}} = \sim 1.18$ – 1.37 $g_{\text{v}} = \sim -0.12$ – -0.28 $m_{\text{n}} = 0.160$ $m_{\text{p}} = 0.6$	$g_{\text{eff}} = 12$ $g_{\text{v}} = 13$ $m_{\text{L,n}} = 0.080$ $m_{\text{L,p}} = 0.105$
Effective mass	$M_{\text{A}} = m_{\text{p}} + m_{\text{n}}$ $= \sim 0.78$ – 0.9 $M_{\text{A}} = m_{\text{p}} + m_{\text{n}} = 3.0$ $= 0.158$ $m_{\text{n}} = 0.210$ $m_{\text{p}} = 0.64$	$m_{\text{n}} = 0.6$ $d_{15} = -10.51$ $d_{31} = -3.93$ $d_{33} = 7.84$	$d_{15} = -4.37$ $d_{31} = -2.14$ $d_{33} = 3.66$ (Zinc) $d_{14} = 3.117$		
Piezoelectric strain coefficient					

Piezoelectric strain coeff. coefficient	$m_n = 0.158$	$d_{15} = -10.51$	$(\text{Hex.}) d_{15} = -4.37$	$(\text{Zinc.}) d_{14} = 1.10$
	$m_p = 0.64$	$d_{31} = -3.93$	$d_{31} = -2.14$	
	$d_{33} = 9.70$	$d_{33} = 7.84$	$d_{33} = 3.66$	
			$(\text{Zinc.}) d_{14} = 3.117$	
<hr/>				
Piezoelectric stress coeff. coefficient		$\epsilon_{15} = -0.138$	$\epsilon_{15} = -0.118$	$\epsilon_{14} = 0.049$
		$\epsilon_{31} = -0.160$	$\epsilon_{31} = -0.238$	
		$\epsilon_{33} = 0.347$	$\epsilon_{33} = 0.265$	
Dielectric constants		$\epsilon(0) = 9.38$	$\epsilon_{14} = 0.140$	
		$\epsilon_{11} = 8.7$	$\epsilon_{11}(0) = 8.31$	$\epsilon(0) = \sim 160-181$
		$\epsilon_{33} = 9.25$	$\epsilon_{33}(0) = 8.76$	$\epsilon(0) = \sim 16.2-18.2$
Nonlinear optical parameters		$\epsilon_{11}(\infty) = 5.53$	$\epsilon_{11}(\infty) = 8.25$	
		$\epsilon_{33}(\infty) = 5.5$	$\epsilon_{33}(\infty) = 8.59$	
		Two-photon absorption coefficient: $K_2 = 0.050$ at $1.06 \mu\text{m}$	Two-photon absorption coefficient: $K_2 = 0.2 \times 10^{-4}$ at $1.06 \mu\text{m}$	Two-photon absorption coefficient: $K_2 = 0.17 \times 10^{-4}$ at $1.06 \mu\text{m}$
		$K_2 = \sim 0.56-0.7$		$K_2 = 0.08 \times 10^{-6}$ at 3.56 eV

1. Effective masses are given in the unit of electron mass, m_0 . The subscripts of the g factor are: v = valence electron, c = conduction electron, \parallel = parallel component, \perp = perpendicular component, n = electron, p = hole. $\epsilon(0)$ = low-frequency dielectric constant, $\epsilon(\infty)$ = high-frequency dielectric constant.

Table 18.9. (cont.).¹

Property	TiO ₂	GaAs	Ge	Si
Lattice parameters (Å)				
	Tetragonal (Anatase) $a = 3.7845$, $c = 9.5143$	Zincblende: stable at normal pressure $a = 5.653$	I: diamond, $a = 5.6579$ II: hex. $a = 4.88$, $c = 2.692$	I: $a = 5.431$ (diamond) II: $a = 4.686$, $a = 2.258$ III: $a = 6.636$ IV: $a = 3.8$, $c = 6.28$
	tetragonal (Rutile) $a = 4.5941$, $c = 2.9589$	Orthorhombic distortion, high-pressure phase $a = 4.946$, $b = 4.638$, $c = 5.493$		
Density (g cm^{-3})	3.894 (Anatase) 4.259 (Rutile)	5.3176	5.3234	I: 2.329
Melting point (K)	Sublime before melting $T_m = 1513$	Sublime before melting $T_m = 1513$	1210	1685
Band gap (eV)	Direct: ~ 3.033 – 3.062 Indirect: ~ 3.049 – 3.101	1.424 (300K)	Direct: 0.805 (293K) Indirect: 0.664 (293 K)	Indirect: 1.110 (300 K) 1.17 (0 K) 1117
Optical absorption edge (nm)	404–408 (direct)	870	1540	1.155 (1.8 k)
Exciton energies (eV)	1.515 (1.8 K)	1.515 (1.8 K)	0.739 (1.7 K)	$g_c = -1.999$
g factor		$g_c = -0.44$ (4 K)	$g_v = -1.8$ (1.7 K) -3.0 (30 K)	
Effective mass		$m_{p,h} = 0.51$ $m_{p,l} = 0.082$ $m_{s,o} = 0.154$ $m_{p,d} = 0.53$	$g_n = 1.5$, $g_p = 3.8$ $m_{n,perp} = 0.0807$ $m_{n,para} = 1.57$	$m_{n,perp} = 0.1905$ $m_{n,para} = 0.9163$ $m_{n,ds} = 1.062$ $m_{n,opt} = 0.43$
Piezoelectric strain coefficient	$d_{11} - d_{12} = 111 \times 10^{-8}$ 3.5 μm $d_{44} = 140 \times 10^{-8}$ 10.39 μm			

$$m_{n,ds} = 1.004$$

$$m_{n,opt} = 0.43$$

$$m_{s,0} = 0.154$$

$$m_{p,d} = 0.53$$

Piezoelectric strain coefficient $d_{11} - d_{12} = 111 \times 10^{-8}$
 $3.5 \mu\text{m}$
 $d_{44} = 140 \times 10^{-8}$
 $10.39 \mu\text{m}$

Dielectric constants

$$\epsilon_{||}(0) = 8.31$$

$$\epsilon_{33}(0) = 8.76$$

$$\epsilon_{||}(\infty) = 8.25$$

$$\epsilon_{33}(\infty) = 8.59$$

$$\epsilon = 12.1 \text{ (4.2 K)}$$

$$\epsilon = 11.9 \text{ (300)}$$

Nonlinear optical parameters

Two-photon absorption
 coefficient: $K_2 = 0.2 \times 10^{-4}$
 at $1.06 \mu\text{m}$

- Effective masses are given in the unit of electron mass, m_0 . The subscripts of the g factor are: v = valence electron, c = conduction electron, $||$ = parallel component, \perp = perpendicular component, n = electron, p = hole. $\epsilon(0)$ = low-frequency dielectric constant, $\epsilon(\infty)$ = high-frequency dielectric constant.

complex interplay between the electron population in the electronic bands, in the traps (whose levels correspond to bulk imperfections), and in the available surface states, in addition to the ongoing interfacial electrochemical and photoelectrochemical processes. The significance of this work is that it has unambiguously demonstrated morphology-dependent spectroelectric, electric, and electrochemical properties of PbS nanocrystallites grown under monolayers [85].

Metals behave like to semiconductors; in the macroscopic regime their properties are size independent, whereas in the nanodomains there is a recognized transition from nonmetallic to metallic behavior [183]. The situation for magnetic, let alone ferroelectric and piezoelectric, materials is more complex and as yet incompletely understood. Such questions as (i) what is the size of the smallest single-domain magnetic (or ferroelectric) particle?, and (ii) what are the properties of size-quantized and dimensionally reduced magnetic (or ferroelectric) particles? have not been adequately answered either theoretically or experimentally.

18.4 Current Trends and Future Directions

An attempt has been made to select contributions in the present book that represent the current trends and future directions in the preparation, characterization, and utilization of nanoparticles and nanostructured films.

Chemists have risen rather successfully to the challenge of making nanoparticles, as evidenced in the present chapter. It is well within their means to prepare dispersions of any desired simple or complex nanoparticles in a high degree of monodispersity. Furthermore, it is often possible to isolate the nanoparticles as solid powders and redisperse them without affecting their sizes and size distributions. Most of these preparations are based on well-established colloid chemical processes. The use of such relatively simple and flexible templates as monolayers (Chapter 2), reversed micelles (Chapter 4) and polymers (Chapter 7) are also based on colloid and surface chemical principles. Similarly, determinations of adsorption isotherms provided [13, 28, 184–189] the information necessary for the characterization of nanoreactors that spontaneously form upon the selective adsorption of a polar liquid onto a solid surface from binary polar–apolar mixtures. Generation of size-quantized semiconductor nanoparticles at dispersed organoclay complexes [13] and layered silicates [28] illustrates the use of the nanophase reactors provided by adsorbed binary liquids. The binary liquid pairs ethanol(1)–cyclohexane(2) and methanol(1)–cyclohexane(2) are highly suitable since the polar component of the liquid mixture (1) is preferentially adsorbed at the solid interface, and hence its mole fraction in the bulk (x_1) is negligible (i.e. $x_1^s \gg x_1$ and $x_2^s \ll x_2$), and since the semiconductor precursors (Cd^{2+} and Zn^{2+}) are highly soluble in the liquid which preferentially adsorbed at the interface (methanol and ethanol), although they are insoluble in the bulk phase (predominantly cyclohexane). These conditions effectively limited the nucleation and growth of the semiconductors to the nanophase reactor provided by the adsorption layer at the solid interface. By varying the mole fraction

of the polar liquid (1) it is possible to control the volume of the nanophase reactor and hence the size of the semiconductor particles grown therein.

Much progress has been made in exploiting such rigid templates as zeolites (Chapter 17), opals (Chapter 13), and porous membranes (Chapter 10) for the preparation of nanoparticles, nanofibrils, and nanotubes. Versatility and reproducibility are distinct advantages of this approach. Electrochemistry is increasingly being employed for the generation of nanoparticles, nanostructured films, and superlattices (Chapters 1 and 3). Indeed, electrodeposition in the cavities of porous membranes can be considered to be a kind of templating in a nanobreaker (Chapter 10).

Nanoparticle research not only benefits from colloid and surface science but also contributes to it. Our need to construct ever more sophisticated supramolecular and heterosupramolecular structures (Chapter 16) demands a better understanding of intricate surface and interparticle colloid chemical interactions and reactions. Thus, it is not surprising that physicists, chemical physicists, and materials scientists are devoting increasingly more attention to the surface and colloid phenomena (Chapters 11 and 12, for example). Their efforts are made easier, of course, by the availability of a large variety of different techniques. Of these, special mention should be made of the surface force apparatus and the scanning force microscope [190–192], which permit both the imaging and the manipulation of nanoparticles and atomic clusters [193, 194] as well as the determination of interparticle interaction forces [195].

Considerable work is being directed toward examining the mechanism of nanoparticle-mediated electron and photoelectron transfers (Chapters 9 and 14). The importance of electrical double layers to electron transfer cannot be overemphasized (Chapter 12). It is quite remarkable that determination of nanoparticle-mediated single-electron transfer events are in our grasp (Chapter 15). This should lead to the fabrication of novel nanodevices.

Many new nanoparticles have been prepared by enterprising chemists. Preparation of porous silicon nanoparticles by a variety of different methods (see Chapters 5 and 8) is particularly significant since they have been shown to undergo photoluminescence and they can be readily integrated into silicon-based integrated circuitry.

Reference should be made to polymeric nanoparticles and dendrimers even though they have not been explicitly discussed in the present volume. Polymeric nanoparticles in the 1–100 nm-size regime, just like their metallic and semiconducting counterparts, exhibit optical and magnetic properties that are different than those observed in the bulk for the same polymers [196, 197]. Dendrimers are characterized by highly branched structures in which all bonds converge to a central core [198]. They are uniform in shape, size, and structure and can be spread on water and aqueous solution surfaces. Dendrimers also display properties that are different than those associated with polymers. These differences manifest themselves in altered chemical reactivities and in distinct nanoenvironments [198]. Many optical and electro-optical [197, 199], as well as biological [200], applications have been found for polymeric nanoparticles. Furthermore, polymeric nanoparticles [201], just like polyelectrolytes [202, 203], have been self-assembled in two-dimensional arrays and three-dimensional superlattices.

In spite of the extremely rapid progress in nanoparticles research, exploitation of the results to practical functioning economic devices has been disappointingly slow. We are confident that we shall witness a rapid progress in this direction in the very near future. The key lies, we believe, in using nanoparticles as molecules and constructing, or preferentially self-assembling, functional three-dimensional networks with a desired composition and topology.

Acknowledgments

We are grateful to the National Science Foundation, which supported most of the experimental work of our group. Janos H. Fendler thanks the donors of the Meyerhof Visiting Professorship for making his stay at the Weizmann Institute of Science, Rehovot, Israel possible and for allowing him to complete the writing of this chapter and the editing of this book. The true credit is due, of course, to the numerous scientists whose creative work has defined and stimulated our progress in nanoparticle research.

References

- [1] D. F. Evans, H. Wennerstrom, *The Colloid Domain. Where Physics, Chemistry and Technology Meet*, VCH, New York 1994.
- [2] G. A. Ozin, *Acc. Chem. Res.* **1997**, *30*, 17–27.
- [3] (a) S. Mann, *Biomimetic Materials Chemistry*, VCH, New York 1996. (b) P. Calvert, P. Rieke, *Chem. Mater.* **1996**, *8*, 1715–1727.
- [4] L. Addadi, S. Weiner, *Angew. Chem. Int. Ed. Eng.* **1992**, *31*, 153–169.
- [5] J. H. Fendler, *Membrane Mimetic Approach to Advanced Materials*, Springer-Verlag, Berlin, 1992.
- [6] J. H. Fendler, F. C. Meldrum, *Adv. Mater.* **1995**, *7*, 607–632.
- [7] A. P. Alivisatos, *Materials Research Society Bulletin* **1995**, *XX*, 23–31.
- [8] A. Henglein, *Ber. Bunseng. Phys. Chem.* **1995**, *99*, 903–913.
- [9] G. Hodes, *Solar Energy Materials and Solar Cells* **1994**, *32*, 323.
- [10] H. Weller, *Angew. Chem. Int. Ed. Eng.* **1993**, *32*, 41–53.
- [11] P. V. Kamat, *Progr. Reaction Kinetics* **1994**, *19*, 277–316.
- [12] M. A. Marcus, W. Flood, M. Steigerwald, L. Brus, M. Bawendi, *J. Phys. Chem.* **1991**, *95*, 1572–1576.
- [13] I. Dekany, L. Turi, E. Tombacz, J. H. Fendler, *Langmuir* **1995**, *11*, 2285–2292.
- [14] A. P. Alivisatos, *J. Phys. Chem.* **1996**, *100*, 13266–13239.
- [15] R. W. Collins, P. M. Fauchet, I. Shimizu, J. C. Vial, T. Shimada, A. P. Alivisatos, *Advances in Microcrystalline and Nanocrystalline Semiconductors*, Materials Research Society, Pittsburgh 1997.
- [16] J. H. Fendler, I. Dekany, *Nanoparticles in Solids and Solutions*, NATO ASI Series, Kluwer, Dordrecht 1996.
- [17] (a) A. Ulman, *Adv. Mater.* **1993**, *5*, 55–57. (b) J. Liu, A. Kim, L. Q. Wang, B. J. Palmer, Y. L. Chen, P. Bruinsma, B. C. Bunker, G. J. Exarhos, G. L. Graff, P. C. Rieke, G. E. Fryxell, J. W. Virden, B. Tarasevich, L. A. Chick, *Adv. Colloid Interface Sci.* **1996**, *69*, 131–180.

- [18] A. Chemseddine, H. Weller, *Ber. Bunseng. Phys. Chem.* **1993**, 97, 636–637.
- [19] T. Vossmeier, L. Katsikas, M. Giersig, I. G. Popovic, K. Diesner, A. Chemseddine, A. Eychmuller, H. Weller, *J. Phys. Chem.* **1994**, 98, 7665–7673.
- [20] C. B. Murray, D. J. Norris, M. G. Bawendi, *J. Am. Chem. Soc.* **1993**, 115, 8706–8715.
- [21] B. O. Dabbousi, C. B. Murray, M. F. Rubner, M. G. Bawendi, *Chem. Mater.* **1994**, 6, 216–219.
- [22] M. Nirmal, C. B. Murray, M. G. Bawendi, *Phys. Rev. B*, **1994**, 50, 2293–2300.
- [23] Y. Nosaka, H. Shigeno, T. Ikeuchi, *J. Phys. Chem.* **1995**, 99, 8317–8322.
- [24] Y. Wang, M. Harmer, N. Herron, *Israel J. Chem.* **1993**, 33, 31–39.
- [25] M. E. Brechley, M. T. Weller, *Angew. Chem. Int. Ed. Engl.* **1993**, 32, 1663–1665.
- [26] N. Herron, J. C. Calabrese, W. E. Farneth, Y. Wang, *Science* **1993**, 259, 1426–1428.
- [27] T. Vossmeier, C. Reck, L. Katsikas, E. T. K. Haupt, B. Schulz, H. Weller, *Science* **1995**, 267, 1476–1479.
- [28] I. Dekany, L. Nagy, L. Turi, Z. Kiraly, N. A. Kotov, J. H. Fendler, *Langmuir* **1996**, 12, 3709–3715.
- [29] Y. A. Barnakov, M. S. Ivanova, R. A. Zvinchuk, A. A. Obryadina, V. P. Petranovskii, V. V. Poborchii, Y. E. Smirnov, A. Shchukarev, Y. V. Ulashkevich, *Inorg. Mater.* **1995**, 31, 752–755.
- [30] G. A. Ozin, *Adv. Mater.* **1994**, 6, 71–76.
- [31] T. Sugimoto, G. E. Dirige, A. Muramatsu, *J. Colloid & Interface Sci.* **1996**, 180, 305–308.
- [32] S. A. Gurevich, A. I. Ekimov, I. A. Kudryavtsev, O. G. Lyublinskaya, A. V. Osinskii, A. S. Usikov, N. N. Faleev, *Semiconductors* **1994**, 28, 486–493.
- [33] S. Y. Chang, L. Liu, S. A. Asher, *J. Am. Chem. Soc.* **1994**, 116, 6739–6744.
- [34] R. A. Hobson, P. Mulvaney, F. Grieser, *J. Chem. Soc., Chem. Commun.* **1994**, 823–824.
- [35] (a) M. Kundu, A. A. Khosravi, S. K. Kulkarni, P. Singh, *J. Mater. Sci.* **1997**, 32, 245–258.
(b) H. Yoneyama, T. Torimoto, *Adv. Mater.* **1995**, 7, 492–494.
- [36] J. L. Coffey, R. R. Chandler, C. D. Gutsche, I. Alam, R. F. Pinizzotto, H. Yang, *J. Phys. Chem.* **1993**, 97, 696–702.
- [37] (a) T. Trindade, P. O'Brien, *J. Mater. Chem.* **1996**, 6, 343–347. (b) T. Trindade, P. O'Brien, *Adv. Mater.* **1996**, 8, 161–163.
- [38] Y. Golan, L. Margulis, G. Hodes, I. Rubinstein, J. L. Hutchison, *Surface Sci.* **1994**, 311, 633–640.
- [39] U. Demir, C. Shannon, *Langmuir* **1994**, 10, 2794–2799.
- [40] S. Gorer, G. Hodes, *J. Phys. Chem.* **1994**, 98, 5338–5346.
- [41] G. Hodes, *Israel J. Chem.* **1993**, 33, 95–106.
- [42] T. Edamura, J. Muto, *Thin Solid Films* **1993**, 226, 135–139.
- [43] S. W. Haggata, X. C. Li, D. J. Cole-Hamilton, J. R. Fryer, *J. Mater. Chem.* **1996**, 6, 1771–1780.
- [44] S. R. Bigham, J. L. Coffey, *Colloids and Surfaces A – Physicochemical and Engineering Aspects* **1995**, 95, 211–219.
- [45] J. Lin, E. Cates, P. A. Bianconi, *J. Am. Chem. Soc.* **1994**, 116, 4738–4745.
- [46] M. Moffitt, A. Eisenberg, *Chem. Mater.* **1995**, 7, 1178–1184.
- [47] M. Moffitt, L. McMahon, V. Pessel, A. Eisenberg, *Chem. Mater.* **1995**, 7, 1185–1192.
- [48] H. Noglik, W. J. Pietro, *Chem. Mater.* **1995**, 7, 1333–1336.
- [49] V. S. Gurin, M. V. Artemyev, *J. Cryst. Growth* **1994**, Sep 13–17, 993–997.
- [50] H. Yao, N. Kitamura, *Bull. Chem. Soc. Jpn.* **1996**, 69, 1227–1232.
- [51] K. M. Choi, K. J. Shea, *J. Phys. Chem.* **1994**, 98, 3207–3214.
- [52] K. M. Choi, K. J. Shea, *Chem. Mater.* **1993**, 5, 1067–1069.
- [53] M. Nogami, A. Kato, *J. Non-Cryst. Sol.* **1993**, 163, 242–248.
- [54] H. Mathieu, T. Richard, J. Allegre, P. Lefebvre, G. Arnaud, *J. Appl. Phys.* **1995**, 77, 287–293.
- [55] T. Fujii, Y. Hisakawa, E. J. Winder, A. B. Ellis, *Bull. Chem. Soc. Jpn.* **1995**, 68, 1559–1564.
- [56] A. Othmani, J. C. Plenet, E. Berstein, C. Bovier, J. Dumas, P. Riblet, P. Gilliot, R. Levy, J. B. Grun, *J. Cryst. Growth* **1994**, 144, 141–149.
- [57] K. M. Choi, J. C. Hemminger, K. J. Shea, *J. Phys. Chem.* **1995**, 99, 4720–4732.
- [58] M. Nogami, A. Kato, Y. Tanaka, *J. Mater. Sci.* **1993**, 28, 4129–4133.

- [59] D. Lincot, R. Ortegaborges, M. Froment, *Philos. Mag. B - Phys. Condens. Matter Struct. Electr. Opt. Magn. Prop.* **1993**, 68, 185-194.
- [60] M. Nogami, A. Nakamura, *Physics and Chemistry of Glasses* **1993**, 34, 109-113.
- [61] J. Butty, N. Peyghambarian, Y. H. Kao, J. D. Mackenzie, *Appl. Phys. Lett.* **1996**, 69, 3224-3226.
- [62] J. Y. Wang, R. A. Uphaus, S. Ameenuddin, D. A. Rintoul, *Thin Solid Films* **1994**, 242, 127-131.
- [63] Y. Golan, J. L. Hutchison, I. Rubinstein, G. Hodes, *Adv. Mater.* **1996**, 8, 631-633.
- [64] (a) S. Mahamuni, A. A. Khosravi, M. Kundu, A. Kshirsagar, A. Bedekar, D. B. Avasare, P. Singh, S. K. Kulkarni, *J. Appl. Phys.* **1993**, 73, 5237-5240. (b) Y. Nosaka, Y. Nosaka, *Langmuir* **1997**, 13, 708-713.
- [65] V. Sankaran, J. Yue, R. E. Cohen, R. R. Schrock, R. Silbey, *J. Chem. Mater.* **1993**, 5, 1133-1142.
- [66] I. Moriguchi, H. Nii, K. Hanai, H. Nagaoka, Y. Teraoka, S. Kagawa, *Colloids and Surfaces* **1995**, 103, 173-181.
- [67] Y. Yang, J. M. Huang, S. Liu, J. Shen, *J. Mater. Chem.* **1997**, 7, 131-133.
- [68] S. Lindroos, T. Kanninen, M. J. Leskela, *Mater. Chem.* **1996**, 6, 1497-1500.
- [69] W. B. Sang, Y. B. Qian, W. M. Shi, D. M. Wang, J. H. Min, W. H. Wu, Y. F. Liu, J. D. Hua, J. Fang, Y. F. Yue, *J. Phys.-Condens. Matter.* **1996**, 8, 499-504.
- [70] G. A. Ozin, M. R. Steele, A. Holmes, *J. Chem. Mater.* **1994**, 6, 999-1010.
- [71] W. Tang, D. C. Cameron, *Thin Solid Films* **1996**, 280, 221-226.
- [72] G. M. Li, M. Nogami, *J. Appl. Phys.* **1994**, 75, 4276-4278.
- [73] D. W. Bahnemann, *Israel J. Chem.* **1993**, 33, 115-136.
- [74] G. Redmond, D. Fitzmaurice, M. Graetzel, *Chem. Mater.* **1994**, 6, 686-691.
- [75] S. Mahamuni, B. S. Bendre, V. J. Leppert, C. A. Smith, D. Cooke, S. H. Risbud, H. W. H. Lee, *Nanostructured Materials* **1996**, 7, 659-666.
- [76] S. Peulon, D. Lincot, *Adv. Mater.* **1996**, 8, 166-170.
- [77] J. Y. Ying, G. McMahon, *Mater. Res. Soc. Symp. Proc.* **1993**, 286, 73-79.
- [78] M. S. El-Shall, W. Slack, W. Vann, D. Kane, D. Hanley, *J. Phys. Chem.* **1994**, 98, 3067-3070.
- [79] X. C. Li, J. R. Fryer, D. J. Colehamilton, *J. Chem. Soc., Chem. Commun.* **1994**, 1715-1716.
- [80] R. Tassoni, R. R. Schrock, *Chem. Mater.* **1994**, 6, 744-749.
- [81] R. S. Kane, R. E. Cohen, R. Silbey, *Chem. Mater.* **1996**, 8, 1919-1924.
- [82] X. Peng, R. Lu, Y. Zhao, L. Qu, H. Chen, T. Li, *J. Phys. Chem.* **1994**, 98, 7052-7055.
- [83] M. Gao, Y. Yang, B. Yang, F. Bian, J. Shen, *J. Chem. Soc., Chem. Commun.* **1994**, 2779-2780.
- [84] J. Yang, J. H. Fendler, H. Janos, *J. Phys. Chem.* **1995**, 99, 5505-5511.
- [85] Y. C. Tian, C. J. Wu, N. Kotov, J. H. Fendler, *Adv. Mater.* **1994**, 6, 959-962.
- [86] J. P. Yang, S. B. Qadri, B. R. Ratna, *J. Phys. Chem.* **1996**, 100, 17255-17259.
- [87] A. J. Ward, E. C. Sullivan, J.-C. Rang, J. Nedeljkovic, R. C. Patel, *J. Colloid & Interface Sci.* **1993**, 161, 316-320.
- [88] T. Takada, T. Yano, A. Yasumori, M. Yamane, *J. Ceramic Soc. Japan* **1993**, 101, 73-75.
- [89] L. Butler, G. Redmond, D. Fitzmaurice, *J. Phys. Chem.* **1993**, 97, 10750.
- [90] S. S. Kher, R. L. Wells, *Chem. Mater.* **1994**, 6, 2056-2062.
- [91] S. S. Kher, R. L. Wells, *Nanostructured Materials* **1996**, 7, 591-603.
- [92] H. Matsumoto, H. Uchida, H. Yoneyama, T. Sakata, H. Mori, *Res. Chem. Intermed.* **1994**, 20, 723-733.
- [93] O. I. Micic, C. J. Curtis, K. M. Jones, J. R. Sprangue, A. J. Nozik, *J. Phys. Chem.* **1994**, 98, 4966-4969.
- [94] (a) H. Uchida, C. J. Curtis, A. J. Nozik, *J. Phys. Chem.* **1991**, 95, 5382-5384. (b) H. Uchida, C. J. Curtis, P. V. Kamat, K. M. Jones, A. J. Nozik, *J. Phys. Chem.* **1992**, 96, 1156-1160.
- [95] O. V. Salata, P. J. Dobson, P. J. Hull, J. L. Hutchison, *Appl. Phys. Lett.* **1994**, 65, 189-191.
- [96] A. J. Nozik, H. Uchida, P. V. Kamat, C. Curtis, *Israel J. Chem.* **1993**, 33, 15-20.
- [97] R. L. Wells, S. R. Aubuchon, S. S. Kher, M. S. Lube, P. S. White, *Chem. Mater.* **1995**, 7, 793-800.
- [98] N. Momen, M. P. Pileni, *J. Phys. Chem.* **1996**, 100, 1867-1873.

- s. *Condens. Matter Struct.*
- 3, 34, 109–113
- Phys. Lett.* **1996**, 69, 3224–
- Solid Films* **1994**, 242, 127–
- 1996**, 8, 631–633.
- . Bedekar, D. B. Avasare,
- o) Y. Nosaka, Y. Nosaka,
- Chem. Mater.* **1993**, 5, 1133–
- awa, *Colloids and Surfaces*
- 131–133.
- , 1497–1500.
- . H. Wu, Y. F. Liu, J. D.
- 504.
- 99–1010.
- , 686–691.
- e, S. H. Risbud, H. W. H.
- 5, 73–79.
- ys. Chem.* **1994**, 98, 3067–
- Commun.* **1994**, 1715–1716
- 1924.
- 1994**, 98, 7052–7055.
- em. Commun.* **1994**, 2779–
- 5511.
- 6, 959–962.
- 7255–17259.
- J. Colloid & Interface Sci.*
- Japan* **1993**, 101, 73–75.
- 10750.
- 3.
- Res. Chem. Intermed.* **1994**,
- t, *J. Phys. Chem.* **1994**, 98,
- 5382–5384. (b) H. Uchida,
- m.* **1992**, 96, 1156–1160.
- s. Lett.* **1994**, 65, 189–191.
- 1993**, 33, 15–20.
- te, *Chem. Mater.* **1995**, 7,
- [99] H. Sato, T. Hirai, I. Komasaawa, *Industrial & Engineering Chem. Res.* **1995**, 34, 2493–2498.
- [100] J. Tanori, T. Gulik-Krzywicki, M. P. Pileni, *Langmuir* **1997**, 13, 632–638.
- [101] J. Tanori, M. P. Pileni, *Langmuir* **1997**, 13, 639–646.
- [102] L. Motte, F. Billodet, M. P. Pileni, *J. Mater. Sci.* **1996**, 31, 38–42.
- [103] O. Horvath, J. H. Fendler, *J. Phys. Chem.* **1992**, 96, 9591–9594.
- [104] I. Ichinose, N. Kimizuka, T. Kunitake, *J. Phys. Chem.* **1995**, 99, 3736–3742.
- [105] K. C. Yi, Ph.D. Thesis, Syracuse University **1994**.
- [106] R. S. Urquhart, D. N. Furlong, H. Mansur, F. Grieser, K. Tanaka, Y. Okahata, *Langmuir* **1994**, 10, 899–904.
- [107] I. Moriguchi, K. Hosoi, H. Nagaoka, I. Tanaka, Y. Teraoka, S. Kagawa, *J. Chem. Soc., Faraday Trans.* **1994**, 90, 349–354.
- [108] Y. C. Tian, C. J. Wu, J. H. Fendler, *J. Phys. Chem.* **1994**, 98, 4913–4918.
- [109] Z. Pan, G. Shen, L. Zhang, J. Liu, *J. Mater. Chem.* **1997**, 7, 531–535.
- [110] J. P. Yang, F. C. Meldrum, J. H. Fendler, *J. Phys. Chem.* **1995**, 99, 5500–5504.
- [111] J. P. Yang, J. H. Fendler, *J. Phys. Chem.* **1995**, 99, 5505–5511.
- [112] Z. Y. Pan, G. J. Shen, L. G. Zhang, Z. H. Lu, J. Z. Liu, *J. Chem. Mater.* **1997**, 7, 531–535.
- [113] F. Grieser, D. N. Furlong, D. Scoberg, I. Ichinose, N. Kimizuka, T. Kunitake, *J. Chem. Soc., Faraday Trans.* **1992**, 88, 2207–2214.
- [114] A. Fojtik, A. Henglein, *Chem. Phys. Lett.* **1994**, 221, 363–367.
- [115] K. A. Littau, P. J. Szajowski, A. J. Muller, A. R. Kortan, L. E. Brus, *J. Phys. Chem.* **1993**, 97, 1224–1230.
- [116] L. E. Brus, P. F. Szajowski, W. L. Wilson, T. D. Harris, S. Schuppler, P. H. Citrin, *J. Am. Chem. Soc.* **1996**, 117, 2915–2922.
- [117] D. Gallagher, W. E. Heady, J. M. Racz, R. N. Bhargava, *J. Mater. Res.*, **1995**, 10, 870–876.
- [118] Y. C. Tian, T. Newton, N. A. Kotov, D. M. Guldi, J. H. Fendler, *J. Phys. Chem.* **1996**, 100, 8927–8939.
- [119] X. G. Peng, T. E. Wilson, A. P. Alivisatos, P. G. Schultz, *Angew. Chem., Internat. Ed. Engl.* **1997**, 36, 145–147.
- [120] D. Lawless, S. Kapoor, D. Meisel, *J. Phys. Chem.* **1995**, 99, 10329–10335.
- [121] P. Pechy, F. P. Rotzinger, M. K. Nazeeruddin, O. K. S. Zakeeruddin, R. Humphry-Baker, M. Gretzel, *J. Chem. Soc., Chem. Commun.* **1995**, 65–66.
- [122] T. Saika, T. Iyoda, T. Shimidzu, *Chem. Lett.* **1993**, 2025–2028.
- [123] I. Willner, Y. Eichen, A. J. Frank, M. A. Fox, *J. Phys. Chem.* **1993**, 97, 7264–7271.
- [124] S. A. Majetich, A. D. Carter, R. D. McCullough, *Mat. Res. Soc. Symp. Proc.* **1993**, 286, 87–92.
- [125] M. Danek, K. F. Jensen, C. B. Murray, M. G. Bawendi, *Chem. Mater.* **1996**, 8, 173–180.
- [126] A. Eychmüller, A. Mews, H. Weller, *Chem. Phys. Lett.* **1993**, 208, 59–62.
- [127] A. Hässelbarth, A. Eychmüller, R. Eichberger, M. Giersig, A. Mews, H. Weller, *J. Phys. Chem.* **1993**, 97, 5333–5340.
- [128] K. Vinodgopal, I. Bedja, P. V. Kamat, *Chem. Mater.* **1996**, 8, 2180–2187.
- [129] T. Cassagneau, G. B. Hix, D. J. Jones, P. Mairelestorres, M. Rhomari, J. Roziere, *J. Mater. Chem.* **1994**, 4, 189–195.
- [130] M. Gandais, M. Allais, Y. Zheng, M. Chamarro, *J. Physique IV Ed. Phys.* **1994**, 47–56.
- [131] V. Sukumar, R. H. Doremus, *Physica Status Solidi B – Basic Research* **1993**, 179, 307–314.
- [132] V. Sukumar, S. C. Kao, P. G. N. Rao, R. H. Doremus, *J. Mater. Res.* **1993**, 8, 2686–2693.
- [133] K. M. Choi, K. J. Shea, *J. Am. Chem. Soc.* **1994**, 116, 9052–9060.
- [134] A. Fernández, A. R. González-Elipse, C. Real, A. Caballero, G. Munuera, *Langmuir* **1993**, 9, 121–125.
- [135] G. Lassaletta, A. Fernandez, J. P. Espinos, A. Gonzalez-Elipse, *J. Phys. Chem.* **1995**, 99, 1484–1490.
- [136] P. Hoyer, R. Konenkamp, *Appl. Phys. Lett.* **1995**, 66, 349–351.
- [137] P. Hoyer, H. Weller, *Chem. Phys. Lett.* **1994**, 224, 75–80.
- [138] W. Choi, A. Termin, M. R. Hoffmann, *J. Phys. Chem.* **1994**, 98, 13669–13679.
- [139] S. T. Martin, C. L. Morrison, M. R. Hoffmann, *J. Phys. Chem.* **1994**, 98, 13695–13704.
- [140] B. O. Dabbousi, M. G. Bawendi, O. Onitsuka, M. F. Rubner, *Appl. Phys. Lett.* **1995**, 66, 1316–1318.

- [141] Y. Nosaka, N. Tohriiwa, T. Kobayashi, N. Fujii, *Chem. Mater.* **1993**, 5, 930-932.
- [142] R. Hutter, T. Mallat, A. Baiker, *J. Chem. Soc., Chem. Commun.* **1995**, 2487-2488.
- [143] K. Kameyama, S. Shohji, S. Onoue, K. Nishimura, K. Yahikozawa, Y. Takasu, *J. Electrochem. Soc.* **1993**, 140, 1034-1037.
- [144] R. P. Andres, J. D. Bielefeld, J. I. Henderson, D. B. Janes, V. R. Kolagunta, C. P. Kubiak, W. J. Mahoney, R. G. Osifchin, *Science* **1996**, 273, 1690-1693.
- [145] K. V. Sarathy, G. U. Kulkarni, C. N. R. Rao, *Chemical Communications* **1997**, 537-538.
- [146] A. P. Alivisatos, P. K. Johnson, X. Peng, E. T. Wilson, J. C. Loweth, P. M. Bruchez, C. P. Schultz, *Nature* **1996**, 382, 609-611.
- [147] C. A. Mirkin, R. L. Letsinger, R. C. Mucic, J. J. Storhoff, *Nature*, **1996**, 382, 607-609.
- [148] N. A. Kotov, I. Dekany, J. H. Fendler, *J. Phys. Chem.* **1995**, 99, 13065-13069.
- [149] J. H. Fendler, N. A. Kotov, I. Dékány, in: *Fine Particles Science and Technology From Micro to Nanoparticles* (Ed.: E. Pelizzetti), Kluwer, Netherlands **1996**, pp. 557-577.
- [150] N. A. Kotov, G. Zavala, J. H. Fendler, *J. Phys. Chem.* **1995**, 99, 12375-12378.
- [151] R. C. Freeman, K. C. Grabar, K. J. Allison, R. M. Bright, J. A. Davis, A. Gruthrie, M. B. Hommer, M. A. Jackson, P. C. Smith, D. G. Walter M. J. Natan, *Science*, **1995**, 267, 1629-1632.
- [152] N. Satoh, H. Hasegawa, K. Tsujii, K. Kimura, *J. Phys. Chem.*, **1994**, 98, 2143-2147.
- [153] (a) N. A. Kotov, F. C. Meldrum, C. Wu, J. Fendler, *J. Phys. Chem.* **1994**, 98, 2735-2738. (b) M. Brust, R. Etchenique, E. J. Calvo, G. J. Gordillo, *J. Chem. Soc., Chem. Commun.* **1996**, 1949-1950.
- [154] Y. C. Tian, J. H. Fendler, *Chem. Mater.* **1996**, 8, 969-974.
- [155] N. A. Kotov, F. C. Meldrum, J. H. Fendler, *J. Phys. Chem.* **1994**, 98, 8827-8830.
- [156] (a) F. C. Meldrum, N. A. Kotov, J. H. Fendler, *J. Phys. Chem.* **1994**, 98, 4506-4510. (b) T. Nakaya, Y. J. Li, K. Shibata, *J. Mater. Chem.* **1996**, 6, 691-697.
- [157] N. A. Kotov, G. Zavala, J. H. Fendler, *J. Phys. Chem.* **1995**, 99, 12375-12378.
- [158] F. C. Meldrum, N. A. Kotov, J. H. Fendler, *Langmuir* **1994**, 10, 2035-2040.
- [159] F. C. Meldrum, N. A. Kotov, J. H. Fendler, *J. Chem. Soc. Faraday Trans.* **1995**, 91, 673-680.
- [160] F. C. Meldrum, N. A. Kotov, J. H. Fendler, *Chem. Mater.* **1994**, 7, 1112-1116.
- [161] C. Natarajan, G. Nogami, *J. Electrochem. Soc.* **1996**, 143, 1547-1550.
- [162] Y. P. Sun, E. C. Hao, X. Zhang, B. Yang, M. Y. Gao, J. Shen, *J. Chem. Soc., Chem. Commun.* **1996**, 2381-2382.
- [163] D. Nesheva, D. Arsova, R. J. Ionov, *Mater. Sci.* **1993**, 28, 2183-2186.
- [164] V. L. Colvin, M. C. Schlamp, A. P. Alivisatos, *Nature* **1994**, 370, 354-357.
- [165] P. Hoyer, N. Baba, H. Masuda, *Appl. Phys. Lett.* **1995**, 66, 2700-2702.
- [166] Q. S. Huo, D. I. Margolese, U. Ciesla, D. G. Demuth, P. Y. Feng, T. E. Gier, P. Sieger, A. Firouzi, B. F. Chmelka, F. Schuth, G. D. Stucky, *Chem. Mater.* **1994**, 6, 1176-1191.
- [167] P. C. Rieke, S. B. Bentjen, *Chem. Mater.* **1993**, 5, 43-53.
- [168] M. Ritala, M. Leskelä, L. Niinistö, P. Haussalo, *Chem. Mater.* **1993**, 5, 1174-1181.
- [169] M. Ritala, M. Leskelä, E. Rauhala, *Chem. Mater.* **1994**, 6, 556-561.
- [170] P. Facci, V. Erokhin, A. Tronin, C. Nicolini, *J. Phys. Chem.* **1994**, 98, 13323-13327.
- [171] A. Jentys, R. W. Grimes, *J. Chem. Soc., Faraday Trans.* **1996**, 92, 2093-2097.
- [172] (a) S. Kohtani, A. Kudo, T. Sakata, *Chem. Phys. Lett.* **1993**, 206, 166-170. (b) N. Serpone, P. Maruthamuthu, P. Pichat, E. Pelizzetti, H. Hidaka, *J. Photochem. Photophys. A*, **1995**, 85, 247-255.
- [173] S. Deki, Y. Aoi, O. Hiroi, A. Kajinami, *Chem. Lett.* **1996**, 433-434.
- [174] T. Isago, S. Sonobe, T. Ohkawa, H. Sunayama, *J. Ceram. Soc. Japan* **1996**, 104, 1052-1055.
- [175] P. Hoyer, R. Eichberger, H. Weller, *Ber. Bunsenges. Phys. Chem.* **1993**, 97, 630-635.
- [176] I. Yu, T. Isobe, M. Senna, *Mater. Res. Bull.* **1995**, 30, 975-980.
- [177] P. Hoyer, *Langmuir* **1996**, 12, 1411-1413.
- [178] T. Torimoto, R. J. Fox, M. A. Fox, *J. Electrochem. Soc.* **1996**, 143, 3712-3717.
- [179] B. I. Lemon, J. T. Hupp, *J. Phys. Chem.* **1996**, 100, 14578-14580.
- [180] I. Moriguchi, H. Maeda, Y. Teraoka, S. S. Kagawa, *J. Am. Chem. Soc.* **1996**, 117, 1139-1140.
- [181] R. J. Tonucci, M. Fatemi, *Appl. Phys. Lett.* **1996**, 69, 2846-2848.

- 1993, 5, 930-932.
 1995, 2487-2488.
 wa, Y. Takasu, *J. Electro-*
 Kolagunta, C. P. Kubiak,
ications 1997, 537-538.
 weth, P. M. Bruchez, C. P.
 , 1996, 382, 607-609.
 13065-13069.
nd Technology From Micro
s. 557-577.
 12375-12378.
 Davis, A. Gruthrie, M. B.
 , *Science*, 1995, 267, 1629-
 1994, 98, 2143-2147.
 n. 1994, 98, 2735-2738. (b)
 oc., *Chem. Commun.* 1996,
 , 98, 8827-8830.
 em. 1994, 98, 4506-4510.
 -697.
 12375-12378.
 2035-2040.
nday Trans. 1995, 91, 673-
 7, 1112-1116.
 550.
hem. Soc., Chem. Commun.
 186.
 354-357.
 2702.
 eng, T. E. Gier, P. Sieger,
r. 1994, 6, 1176-1191.
 93, 5, 1174-1181.
 51.
 , 98, 13323-13327.
 2093-2097.
 , 166-170. (b) N. Serpone,
m. Photophys. A, 1995, 85,
 34.
pan 1996, 104, 1052-1055.
 1993, 97, 630-635.
 3, 3712-3717.
em. Soc. 1996, 117, 1139-
 [182] V. Lakhota, J. M. Heitzinger, A. H. Cowley, R. A. Jones, J. G. Ekerdt, *Chem. Mater.* 1994,
 6, 871-874.
 [183] A. Henglein, *Berichte Der Bunsen-Gesellschaft - Physical Chemistry Chemical Physics* 1995,
 99, 903-913.
 [184] I. Dékány, in: *Fine Particle Science and Technology from Micro to Nanoparticles* (Ed.:
 E. Pelizzetti), Kluwer, Netherlands 1996, pp. 293-322.
 [185] I. Dékány, L. G. Nagy, G. Schay, *J. Colloid and Interface Sci.* 1978, 66, 197-199.
 [186] I. Dékány, F. Szántó, A. Weiss, G. Lagaly, *Berichte der Bunsen-Gesellschaft für Physikalische*
Chemie 1985, 89, 62-67.
 [187] I. Dékány, F. Szántó, A. Weiss, G. Lagaly, *Berichte der Bunsen-Gesellschaft für Physikalische*
Chemie 1986, 90, 427-431.
 [188] I. Dékány, F. Szántó, A. Weiss, G. Lagaly, *Berichte der Bunsen-Gesellschaft für Physikalische*
Chemie 1986, 90, 422-427.
 [189] I. Dékány, F. Szántó, A. Weiss, *Colloids and Surfaces* 1989, 41, 107-121.
 [190] J. N. Israelachvili, *Chemtracts - Analytical and Physical Chemistry* 1989, 1, 1-12.
 [191] P. M. Claesson, T. Ederth, V. Bergeron, M. W. Rutland, *Advances in Colloid and Interface*
Science 1996, 119-183.
 [192] M. C. Lieber, J. Liu, P. E. Sheehan, *Angew. Chemie, Int. Edn. English* 1996, 35, 687-704.
 [193] W. A. Hayes, H. Kim, X. H. Yue, S. S. Perry, C. Shannon, *Langmuir* 1997, 13, 2511-2518.
 [194] D. M. R. Kolb, T. Will, *Science* 1997, 275, 1097-1099.
 [195] Y. K. Leong, D. V. Boger, P. J. Scales, T. W. J. Healy, *Colloid and Interface Sci.* 1996, 181,
 605-612.
 [196] D. Y. Godovski, Y. K. P. V. P. E. Godovsky, *Advances in Polymer Science*, 1995, 119, 79-
 122.
 [197] C. Barbero, R. Kötz, *J. Electrochem. Soc.* 1994, 141, 859-865.
 [198] J. M. J. Frechet, C. J. Hawker, I. Gitsov, J. W. J. Leon, *Macromolecular Sci. - Pure and*
Applied Chemistry 1996, a33, 1399-1425.
 [199] M. Granstrom, M. Berggren, O. Inganas, *Science* 1995, 267, 1479-1481.
 [200] S. Margel, I. Burdygin, V. Reznikov, B. Nitzan, O. Melamed, M. Kedem, S. Gura, G.
 Mandel, M. Zuberi, L. Boguslavsky, in *Recent Research Developments in Polymer Science*
 (Ed.: S. G. Patidali), Transworld Research Network 1997.
 [201] O. Karthaus, K. Ijro, M. Shimomura, *Chemistry Letters* 1996, 821-822.
 [202] L. H. Radzilowski, B. O. Carragher, S. I. Stupp, *Macromolecules* 1997, 30, 2110-2119.
 [203] G. Decher, in: *Comprehensive Supramolecular Chemistry*, Vol. 9 (Ed.: J.-P. Sauvage),
 Pergamon, Oxford 1996, pp. 507-528.